SEARCH RADAR

Search radar is used widely to provide electronic surveillance of the environment to detect objects that would otherwise be invisible to the unaided observer. These systems usually function without operator interaction to provide information rates commensurate with high-speed decision making by the user. That user might, for example, be an automated weapon launch system, an air traffic controller, or a traffic policeman.

OVERVIEW

This section provides a summary of the function, applications, elements, and design challenges of modern search radar.

Function

The single function of the radar is to provide *volume surveillance* over all or portions of a sphere centered at the radar antenna. This is accomplished by radiating high-energy microwave pulses into the volume and detecting these pulses as they are reflected from objects of interest (targets). An antenna focuses the radiation to create a narrow beam of energy. This selectivity and the short duration of the pulses allow the radar to measure target location in distance (range) and in one or two angular dimensions (bearing and elevation). The antenna may be rotated mechanically in angle or the beam may be steered electronically in one or two dimensions.

A receiver amplifies the target-reflected pulses and removes the microwave carrier frequency through a heterodyning process. The received pulses are applied to a signal processor for target detection and location measurement. In modern designs, the signals are converted to digital format with subsequent processing carried out digitally.

Target detection is performed by comparing the magnitudes of received signals to a preset threshold. Signals exceeding this threshold are declared targets and their parameters are passed on to a location measurement process. Occasionally, internal receiver noise will exceed threshold. These occurrences are termed false alarms. Adaptive thresholds are employed to maintain a constant average false alarm rate (CFAR).

Target range is determined by noting the time of detection relative to the time of transmission. The translation from time to range is predicated on the fact that the pulses travel at the speed of light. Angular measurement is obtained by noting the position of the antenna at the time of detection.

In simpler applications, target information is applied to an electronic display. This display provides the operator with a picture of the environment that is updated on each antenna scan. Usually, a plan view is presented in x and y coordinates.

Automatic designs rely on a general-purpose digital computer to interpret target detection information. This computer provides scan-to-scan correlation, trajectory extrapolation, and, in military applications, threat assessment. In applications supporting weapon engagement, a kill assessment function may be provided.

In earth-based applications, there are a number of extraneous signals that may cause interference. Among these are unwanted clutter returns from the local terrain, sea surface, or weather. In military applications, an adversary may radiate noise in an attempt to hide returns from their own vehicles. These interference signals are referred to as electronic countermeasures (ECM) or jamming. More sophisticated techniques are in use that attempt to confuse the radar by generating false targets. Finally, a large number of radar systems are in use today. Each has its own peculiar function and set of parameters, but there may be several systems colocated in the same general area. Direct reception of radiation from another radar may be interpreted as a target return. A function of the well-designed radar is minimization of clutter, ECM, and friendly interference effects.

Applications

There are a number of ways to categorize search radars. They may be developed for the military, be produced commercially, or be sponsored by governmental agencies. The platforms may be surface-based at sea or on land, airborne in aircraft or missiles, or space-based. A radar is either two-dimensional (range and bearing) or three-dimensional (range, bearing, and elevation). It also may be characterized, loosely, as long, medium, or short range. Finally, microwave transmission frequency is an important attribute. Radars are in use having carrier frequencies from 1 GHz, or lower, to 20 GHz, or higher.

Examples of search radar applications include general surveillance, weapon support, aircraft and ship navigation, air traffic control, harbor traffic control, early warning of attack, weather alerting and monitoring, obstruction alerting, vehicular speed measurement, and satellite location monitoring.

Elements

In general, a search radar is composed of several distinct electronic elements having specific functions. These include a frequency synthesizer, a timing generator, a power amplifier, an antenna, an antenna platform, a microwave receiver, an intermediate frequency receiver, a signal processor, and a control computer. An operator display-and-control panel may be included. Figure 1 is a block diagram showing the interactions among these elements.

The *frequency synthesizer* provides the basic radar signals necessary for carrier transmission and for local oscillator production. Each frequency conversion used in the radar receivers requires one local oscillator signal. An additional signal may be provided to serve as the basic system clock, which sets the timing intervals for pulse transmission, range gating, and digital sampling. Coherency is an absolute requirement in modern designs due to the need to reject clutter by Doppler processing. Therefore, all signals must be phase related. Often, coherency is controlled by starting with crystal-based oscillators operating at low frequency. Microwave signals are produced using frequency multiplier chains, offset modulators, and frequency dividers.

A *timing generator* provides timing commands for the other radar elements. These commands include transmission pulse width and repetition frequency, range gate width, and digital converter sampling intervals. This element also provides start-and-stop events for the various algorithms involved in signal processing. In designs using phase-steered antennas, the timing generator provides beam-steering commands.

High-power microwave transmission is accomplished using a *power amplifier.* This element amplifies a low-level continuous-wave input from the synthesizer into a high-power pulsed signal for subsequent application to the radiating antenna. Peak power output may range from a few watts to several megawatts and pulse widths from tens of nanoseconds to several microseconds. In long- and medium-range applications, the amplifier will be a vacuum tube. Popular choices for this device are the klystron and the traveling wave tube. The latter is a broadband device suitable for frequency-agile operation. Solid-state devices are available for short-range designs where power levels below approximately 100 W are acceptable. Pulsed operation is provided by a modulator that controls the tube beam current in vacuum tube designs.

The *antenna* functions to focus microwave energy into a narrow spatial beam. In the simpler designs, this device is a parabolic reflector having a feed horn mounted near its focal point. In Cassegrain designs, the feed is located behind the reflector and illuminates a subreflector mounted near the focal point. A more advanced approach uses a slotted waveguide array. Each slot is a sub-radiator and a beam is formed owing to the phase relationship among the slots. In the ultimate design, phase shifters are added to groups of slots to enable electronic beam steering. Advanced designs may add transmit-and-receive modules to slot groups. This approach obviates the necessity for a separate power amplifier.

An *antenna platform* provides mechanical beam rotation and beam stabilization relative to the horizon. Land-based applications require only beam rotation. However, in ship-based or airborne designs, the three-dimensional motion of the host vehicle may dictate gimballing in one or two dimensions in order to maintain a constant geometrical reference. Beam stabilization is afforded using feedback control based on attitude sensors.

The primary functions of the *microwave receiver* include receiver protection from the high-level transmission, frequency selectivity to minimize external interference, and at least one frequency conversion. Some designs also include radar frequency amplification to minimize the loss associated with frequency conversion and to establish a basic system noise figure. Usually, receiver protection is provided by a circulator device that depends on pathlength differentials to cancel the transmission while providing an unattenuated path for target reception. Passive or active limiters are also in use. In modern designs, the receiver is solid state and based on microwave integrated circuit (MIC) technology.

The *intermediate frequency* (IF) *receiver* provides further amplification and frequency conversion of the target returns. It also applies frequency selectivity to pass the pulse spectrum while rejecting unwanted interference. Usually, the final conversion is to video where only a pulsed, Doppler-shifted carrier remains. At that stage, the receiver implements an approximation to a matched filter that maximizes the signal-to-noise ratio. In modern designs, the last element is an analog-to-digital converter that outputs digitized words representing the voltages of incoming signals and noise. Word lengths may vary from eight bits in simpler designs to as many as sixteen bits in advanced applications. The receiver may employ an IF limiter to prevent large clutter returns from saturating the digital converter.

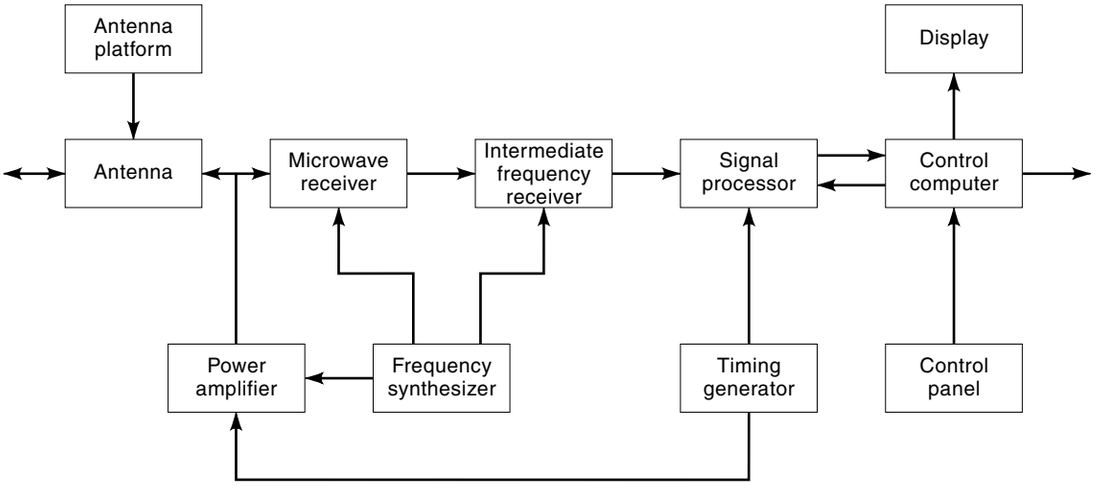

Figure 1. Generalized block diagram of a search radar showing interfaces between elements. Most modern search radars employ the generic elements shown in this diagram.

All decision-making algorithms such as noise estimation, target detection, clutter rejection, and parameter measurement are assigned to the *signal processor.* In modern designs, this element takes the form of a real-time, special-purpose digital computer. It is always solid state and may employ very large-scale integrated (VLSI) circuits to provide ultra-high-speed operation in a small volume. Often, algorithms are hard-wired to perform specific operations but, in some cases, more general purpose, programmable microprocessors are used.

In automatic systems, all basic radar functions are controlled by a general-purpose digital computer. This *control computer* provides radar frequency, pulse width, and repetition frequency commands to the radar transmitter elements, beam steering and rotation rate commands to the antenna elements, and parameter boundaries to the receiver and signal processing elements. This element also receives direct outputs from the signal processor, which it uses to refine target correlation, location measurement, trajectory prediction, threat assessment, and, possibly, kill assessment. In modern designs, this computer is programmable in some higher order language (HOL) such as ADA to provide design flexibility and ease of modification.

Systems dependent upon operator control use a computer of lesser complexity. These systems employ a *control panel* from which the operator enters basic commands to the radar. These may include radar frequency selection, pulse width, repetition frequency, beam control, scan rate, nonradiate sector cutouts, range boundaries, minimum velocity limits, and detection threshold. Radar outputs are sent to a *display.* Detected targets are shown as dots of various intensities located proportionally to target range and bearing. Codes may be attached to designate target type and/or priority. Separate digital readouts may be provided giving more accurate target location data and other pertinent information.

Design Challenges

The designers of a modern search radar system face a number of challenges that must be met to ensure specification compliance and cost effectiveness.

Modern radar is dependent on the phenomenon of Doppler shift to provide a distinction between near-zero velocity clutter and higher velocity targets. Advantage of this phenomenon can be taken only if the transmission and local oscillator signals are coherent. That is, their frequency and phase must remain nearly constant over time. Therefore, close attention must be given to short-term phase and frequency stability. In addition, the high population density of radar in operation forces a tight spectral allocation to each system. Legally, the designer cannot allow his frequency to drift outside the prescribed boundaries. This problem may be resolved by utilizing oscillators based on crystalline structures having a precise molecular structure that supports only a narrow vibration spectrum. Power amplifiers exhibiting low phase noise characteristics may also be required.

Very-short-term instability is referred to as frequency modulation (FM) noise. This noise is usually broadband and is radiated in conjunction with the transmission carrier. Clutter-reflected returns of this noise can cause interference with the relatively low-strength returns from targets even though targets and clutter are separated by a Doppler shift. In typical applications, this noise must be maintained as low as 120 dB below the carrier level when measured in a bandwidth of 1 Hz. Control of this noise may be achieved using automatic phase and frequency control loops within the *frequency synthesizer.*

A coherent radar is dependent upon the stability of the pulse repetition frequency. Deviations in this frequency, termed *pulse jitter,* can cause intermodulation products or clutter to spill over into the target spectrum and cause interference. Careful attention to the stability of the system clock can minimize this problem.

Target detectability is a direct function of transmitted power level. Once a power amplifier device, modulator, and power supply have been selected, this parameter is set. However, care must be taken that its value does not deteriorate over time.

In longer range applications, the transmission power is high enough to destroy receiver circuitry if allowed to enter. It is mandatory that provisions be made to prevent this occurrence. Common practice is to use high power circulator devices whose phase characteristics cause transmission cancellation at the receiver input. In reality, these devices provide

only approximately 20 dB of attenuation. If more isolation is required, active transmit–receive circuitry may be required. These devices are switches that turn off during pulse transmission and turn on afterward to receive signals. High-power passive limiters are also in use. These do not require external timing control. In any case, it is ordinarily not possible to process target returns during the time of pulse transmission. This must be accounted for in terms of the blind range effect on minimum detectable target range, periodic blind range zones, and range ambiguity resolution.

Target detectability, apart from clutter effects, is a direct function of antenna gain. Gain is the ratio of the power density achieved on boresight to that given transmission isotropically into a sphere. Gain is directly proportional to antenna physical area. The design challenge is to find sufficient space to install a large physical item. Long range search antennas may have dimensions measured in meters. Where space limitations exist, trade-offs must be made among transmission power, gain, and receiver sensitivity to achieve an optimum design.

Radar antennas exhibit spatial sidelobes. These lobes allow for leakage into every portion of the radiated sphere and allow for low-level reception from all objects within the sphere. Except for possible clutter degradation and large-target angular measurement, the real concerns are off-axis jamming and friendly interference. Some sidelobe control is always advisable. This is achieved by shaping the illumination current distribution across the antenna face. A uniformly illuminated aperture exhibits a first sidelobe only 13 dB below the main beam gain. Through careful design, this may be increased to 30 dB or more. The penalty for sidelobe control is decreased gain and increased beamwidth. Military, ground-based radars also commonly employ sidelobe cancellers, which are circuits capable of attenuating interference signals from discrete sources.

Antenna beam scan rate is a parameter subject to optimization and trade-off when mechanically scanned antennas are employed. High scan rates yield short target beam dwell times that deprive the radar of available energy and reduce signal-to-noise ratio (SNR). Low scan rates increase the time interval between initial detection and verification detection. Thus, longer detection ranges may be required. Increased range also reduces SNR.

The problem of scan rate optimization is compounded when phase-steered antennas are used. In these systems, the beam may be programmed to scan back to the angle of initial detection immediately for a second detection verification.

Thermally induced receiver noise exists in all radars. Reliable detection and parameter measurement are possible only when target signal levels exceed noise by at least a factor of ten. The careful design will include only those electronic devices having a low noise figure. Noise figure is defined as the ratio of input SNR to output SNR and is a direct measure of degradation due to noise. SNR is also reduced by losses inherent in wave guide runs, coaxial cable runs, connectors, and discrete microwave components. There will also be a loss when the angle of the antenna beam center does not coincide with the actual target angle. Signal processing can also contribute to the loss structure. These include analog-to-digital converter quantization, imperfect thresholding, range gate straddling, and Doppler filter straddling. All of these losses must be kept to a minimum.

Dynamic range is a measure of the radar's ability to process large signal returns simultaneously with very low signal returns without degradation. Generally, clutter returns are the largest signals present at the radar input. If a clutter echo arrives in time conjunction with a target echo and if the clutter level causes receiver saturation, then small signal suppression occurs and target detectability is degraded. Similarly, clutter may exceed the dynamic range of the analog-to-digital converter. In this case, totally erroneous data may be produced. The careful designer will choose analog components having a high saturation level and will choose digital converters having a large number of bits in their output word length. Typically, word lengths of 14 to 16 bits are required to withstand worst-case clutter inputs.

Even when clutter returns are processed linearly through the radar receiver and digital converter, they must be rejected within the signal processor to avoid interference with target returns. Classical analog filtering is not effective against clutter, because the receiver must pass the entire pulse spectrum of the target, typically several megahertz, while the Doppler offset is only on the order of a few kilohertz. Common practice is to employ digital clutter cancelers also known as moving target detectors (MTD). In its simplest form, the MTD algorithm provides subtraction of the current pulse sample from that received one or more repetition intervals earlier. Because clutter has a near-zero Doppler shift, it is canceled almost totally, whereas the Doppler shifted target return is passed with little attenuation. The result is a high-pass digital filter. Feed-forward and feedback multiplication factors may be used to tailor the frequency response to specific target requirements.

Clutter may be received from the terrain, from the surface of the sea and from rainfall. Terrain reflections are usually the most intense, but, because their Doppler shift is very low, they are canceled easily. Sea clutter becomes a problem only under heavy-sea conditions. Rain clutter presents the greatest challenge, because it can be highly intense and that intensity increases with the fourth power of radar frequency. This problem is burdened by the Doppler shifts from wind-driven rain drops. Because wind velocity generally increases with altitude, the cancellation of higher altitude rainfall clutter becomes problematic.

Microwave transmissions tend to resonate with molecules present in the atmosphere. This resonance causes attenuation with an attendant degradation to target detectability. Oxygen and water vapor are the primary contributors to this attenuation, although smoke, haze, and smog can also be factors. Even though there exist windows of decreased attenuation, the effect is more pronounced at higher radar frequencies. Rainfall also can cause severe attenuation. Over frequency, attenuation rates vary from a few tenths of a decibel per kilometer of transmission path to more than 1 dB.

Microwave components contribute some degree of loss with attendant transmission strength reduction and target signal attenuation. Included are waveguide runs, waveguide joints, circulators, phase shifters, limiters, and filters. Without careful design, the summation of these losses can exceed 10 dB.

There are a number of variable losses associated with the antenna beam and signal processing. A target may appear at an angle off the antenna elevation boresight. During the target dwell, the antenna gain will vary. Pulse returns may be sampled at other than peak response times. Noise level estimates may not be exact. The matched filter approximation

used will not yield the theoretical maximum SNR. These effects are always probabilistic but must be considered in detection calculations.

In military applications, ECM must be considered. This is employed in an attempt to hide the echo from incoming aircraft or missiles or to decoy and confuse the search radar. The simplest form is barrage noise jamming in which high noise levels are radiated across the entire frequency band allocated to the radar. These systems require no knowledge of the exact transmission frequency of the victim radar. In those cases where the adversary is able to measure the transmission frequency, spot jamming may be effective. Here, the noise jamming is restricted to the instantaneous spectrum occupied by the radar transmission and may have much higher power density than that of barrage jamming. More advanced techniques are available in which the ECM system reradiates the transmission with variable delay or modulation in an attempt to create false targets. The effectiveness of ECM depends upon whether or not the jamming source can be located in angular coincidence with protected targets. If not, its effect may be minimized by careful control of antenna sidelobes.

Worldwide, there exist a large number of radars of various types operating in a variety of frequency bands. It is likely that a given radar will be required to operate in an environment containing several other radars operating in proximity. In this case, reception of direct transmission and target reflected echoes can cause interference and false target production. When the various radars are of the same type, based on a common design, the designer may minimize interference using careful frequency channelization and repetition frequency selection. When disparate types are involved, techniques exist for editing out pulse returns at repetition frequencies other than that currently used by the victim radar. In all cases, careful antenna sidelobe control is mandatory.

An emerging technology has been deployed that attempts to render aircraft, missiles, and ships invisible to radar. This *stealth technology* utilizes radar absorbent material (RAM) and geometric vehicle design to greatly reduce radar reflectivity. In fact, stealth techniques do not result in total invisibility but radar return levels from these targets are reduced appreciably. Unfortunately, from a design standpoint, little can be done to counter these threats except to increase transmitter power, frequency stability, antenna aperture, and/or receiver sensitivity. However, the stealth technology is not totally effective over an infinite bandwidth. Therefore, it may turn out that the next generation radar designs must be based on either very low or very high radar frequencies. These decisions will have far-reaching implications in terms of antenna beamwidth, Doppler resolution, and repetition frequency selection. Stealth is, probably, the most serious concern for future military radar development.

Target detection decisions are based on signals exceeding some preset threshold. Ideally, that threshold is computed by multiplying an average measurement of the ambient receiver noise level by some constant. Thus, the threshold will vary as the noise level varies due to temperature changes and local clutter conditions. Since false alarms on noise are probabilistic events, this method ensures a constant average false alarm rate (CFAR). The problem is in determining the ambient noise level. This may be accomplished by averaging a number of samples taken from range cells next to the target cell under investigation. Use of a larger number of cells reduces the measurement error but introduces other errors due to the range dependency of clutter.

Once an acceptable false alarm rate is established, the probability of target detection as a function of SNR is computed easily. However, the detection decision need not be based solely on the result of one received pulse. Rather, it should be based on the preponderance of evidence from a group of pulses representing an antenna beam dwell. This evaluation is termed *pulse integration.* It can yield a significant increase in effective SNR.

The accuracy of range measurement is a function of transmitted pulse width. However, when peak power is fixed, short pulses result in lower energy and reduced SNR. Often, pulse compression techniques are employed in which phase coding is applied to subpulses within a longer pulse on transmission. Decoding on reception results in an output pulse width equal to the subpulse but with energy increased by the compression factor. This technique is especially useful in longer range applications where low repetition frequencies are required. Further accuracy may be obtained using split-range gating. In this approach, magnitudes of adjacent range samples are used to form a weighted average proportional to true range. The accuracy of this method improves as SNR increases.

Bearing measurement accuracy is dictated by the azimuth beamwidth of the antenna pattern. In the simplest case, target bearing is assumed equal to the physical angle of boresight at the time of detection. Improved accuracy may be obtained by noting the beginning start and stop angles at the end of above threshold intervals. More advanced designs may use weighted averages of return samples and curve fitting to known antenna beam parameters to increase accuracy. Measurement errors decrease as SNR increases.

In elevation, measurement accuracy is a sole function of elevation beamwidth. In electronically beam-steered applications, where the beam transitions the target vertically as well as horizontally, beam splitting can be used to improve accuracy. Monopulse techniques, commonly used in tracking radars, may also be used in search radars. In these systems, sum and difference beams are formed and processed in separate receiver channels. The voltage ratio between these channels is proportional to target angle in one or two planes.

Except in applications using very low repetition frequencies, initial range measurement is always ambiguous. That is, the true target time delay is equal to the time delay between transmission and detection plus an integral number of repetition intervals. This ambiguity may be resolved by obtaining detections on two or more distinct repetition frequencies.

Final radar computer outputs may include target trajectory prediction, threat assessment, and kill verification. All of these functions are dependent upon radar measurement accuracy. The number and types of algorithms possible are limitless. Development of these algorithms will occupy a large portion of the designer's efforts.

DESIGN CONSIDERATIONS

This section addresses the methodology and mathematics currently used in the development of search radars.

Radar Range Equation

The design of any search radar begins with the *radar range equation.* This equation ties together all major radar parame-

ters into a single relation that enables the computation of SNR. The latter is the single parameter that dictates radar performance both in detectability and in measurement accuracy. Because matched filter theory shows that the maximum SNR achievable is equal to the pulse *energy-to-noise power density ratio* (ENR), it is usual to begin with the following equation.

$$\text{ENR} = \frac{P_t \delta_t G_t \sigma_t A_r N_p L}{(4\pi)^2 R^4 \eta F}$$

where P_t is peak transmitted power, δ_t is pulse width, G_t is transmit antenna gain, σ_t is target cross section, A_r is antenna capture area, N_p is the number of pulses available during the target dwell, L is the system losses, R is target range, η is receiver noise power density, and F is receiver noise figure. Skolnik (1) gives a derivation of the basic equation.

The basic equation may be modified to reflect more germane parameters by substituting various relations among the parameters. The number of pulses available is given by

$$N_p = \frac{T_d}{T_r}$$

where T_d is the dwell time and T_r is the repetition interval. The transmit antenna gain may be expressed as

$$G_t = 4\pi / \theta_a \theta_e$$

where θ_a is the azimuth beamwidth and θ_e is the elevation beamwidth both expressed in radians. Beam dwell time is given by

$$T_d = \theta_a / \omega$$

where ω is the antenna azimuth scan rate. The average transmitted power is

$$P_a = P_t \delta_t / T_r$$

Scan rate is related to single revolution scan time, T_s, as

$$\omega = 2\pi / T_s$$

Elevation beamwidth is given by

$$\theta_e = \phi_e / N_b$$

where ϕ_e is the required elevation angular coverage and N_b is the number of elevation beams used in the search pattern. Finally, the total volume search time is

$$T_v = N_b T_s$$

Insertion of these relations into the original range equation yields the following form, which highlights the critical radar parameters:

$$\text{ENR} = \frac{P_a \sigma_t A_r L T_v}{8\pi^2 \phi_e \eta F R^4}$$

Power-Aperture Product

The designer has control over some parameters but not others. Target cross section and elevation coverage are fixed by system requirements, whereas noise power density must obey the laws of physics. Of the remainder, the designer may choose values of average power and antenna area while minimizing system losses and receiver noise figure. Of most importance is the product of average power and area. This product is termed the *power-aperture product,* and its value dictates directly the performance of the radar.

Two parameters remain. These are volume search time and target range. These are subject to optimization.

Optimum Scan Rate and Instrumented Range

There will be a system requirement on the minimum acceptable detection range. In military applications, weapon response times dictate this range. In nonmilitary systems such as airport traffic control, there exists a desired minimum range so that traffic may be diverted or altered to ensure safe arrival of all aircraft. Let the minimum range be denoted R_d.

The search radar requires a finite time to search its entire designated volume. It is possible that the last opportunity for detection occurs at the leading edge of this search time. The corresponding initial range is

$$R_i = R_d + V_t T_v$$

where V_t is target incoming velocity. If detection does not occur at that range, the next opportunity may be inside the minimum range.

The ENR at initial range is given by

$$\text{ENR} = \frac{P_a \sigma_t A_r L}{8\pi^2 \phi_e \eta F} \cdot \frac{T_v}{(R_d + V_t T_v)^4}$$

It seems reasonable to maximize ENR at the initial detection range. That occurs when the rightmost factor, involving T_v, is maximum. That maximum is found by differentiation. The result shows an optimum search time given by

$$T_v = R_d / 3V_t$$

Substitution of this value gives the optimized initial range as

$$R_i = \tfrac{4}{3} R_d$$

This is the well known $\frac{4}{3}$ law of search radar design.

Define

$$k = 3^3 / 4^4 8\pi^2$$

Then, maximized ENR at initial range is given by

$$\text{ENR} = \frac{k P_a \sigma_t A_r L}{\phi_e \eta F V_t R_d^3}$$

This final form of the range equation shows the importance of power-aperture product and the impact of system design requirements. It is to be noted that, in this form of the range equation, ENR is inversely proportional to the third power of range, whereas the standard form suggests a fourth power dependency.

Preliminary Design Example

Manipulation of the radar range equation is such an integral part of the preliminary design process that an example is warranted.

Solving the previous equation for power-aperture product gives

$$P_a A_r = \frac{\text{ENR} \cdot \phi_e \eta F V_t R_d^3}{k \sigma_t L}$$

Suppose requirements are that the elevation coverage be 45 degrees (0.785 rad), the maximum target velocity is 1100 m/s, the desired declaration range is 10 km, and the minimum target cross section is 0.01 m^2.

Usually, range equation parameters are tabulated in terms of decibels. Power levels are expressed in decibels relative to one milliwatt (dB/mW). Furthermore, assume that the receiver noise figure is 3.0 dB and that the total system losses are 10.0 dB. Also, assume that an ENR of 13.0 dB provides adequate detectability and accuracy. Noise power density is fixed at −174.0 dB relative to 1 mW/Hz and the constant, k, reduces to −28.7 dB.

These parameters are listed in Table 1 and the required power-aperture product is computed.

Therefore, the required power-aperture product is 50 $\text{dB/mW} \cdot \text{m}^{-2}$.

Suppose that a 1 m^2 antenna fits the available volume constraints. Then, the required average transmitted power is 50 dB/mW or 100 watts. Now, the designer may work backward to find appropriate values for the other pertinent parameters.

Assume that a pulse width of 200 ns is desired for range accuracy and that a repetition interval of 10 μs is acceptable from an ambiguity resolution standpoint. These decisions dictate a peak transmitted power of

$$P_t = \frac{P_a T_r}{\delta_t} = \frac{10^5 \times 10 \times 10^{-6}}{200 \times 10^{-9}} = 5 \times 10^6 \text{ mW}$$

or 5 kW (67 dB/mW).

The optimized volume search time is

$$T_v = \frac{R_d}{3V_t} = \frac{10,000}{3 \times 1100} = 3 \text{ s}$$

Suppose that elevation accuracy requires four elevation beams. Then, the single revolution scan time is

$$T_s = \frac{T_v}{N_b} = \frac{3}{4} = 0.75 \text{ s (80 RPM)}$$

Table 1. Example of Computation of Required Power-Aperture Product

Parameter	dB
ENR	13.0
ϕ_e	−1.0
η	−174.0
F	3.0
V_t	30.4
R_d^3	120.0
k	28.7
σ_t	−20.0
L	10.0
$P_a A_r$	50.1

The resulting elevation beamwidth is

$$\theta_e = \frac{\phi_e}{N_b} = \frac{45}{4} = 11.25 \text{ deg (0.196 rad)}$$

The antenna scan rate is

$$\omega = \frac{2\pi}{T_s} = \frac{2\pi}{0.75} = 8.38 \text{ rad/s}$$

Antenna gain is related to aperture area as

$$G_t = \frac{4\pi A_r}{\lambda^2}$$

where λ is the wavelength. Wavelength is related to radar frequency, F_r, as

$$\lambda = c/F_r$$

where c is the velocity of propagation (3.0×10^8 m/s). Assume that this radar has been assigned to operate in the X-band at F_r = 10 GHz. Then, the wavelength is

$$\lambda = \frac{3.0 \times 10^8}{10 \times 10^9} = 0.030 \text{ m}$$

and the resulting antenna gain is

$$G_t = \frac{4\pi}{(0.030)^2} = 13,963 \text{ (41.4 dB)}$$

From the gain, azimuth beamwidth may be computed. Thus,

$$\theta_a = \frac{4\pi}{G_t \theta_e} = \frac{4\pi}{13963 \times 0.196} = 0.004459 \text{ rad (0.26 deg)}$$

The azimuth dwell time is

$$T_d = \frac{\theta_a}{\omega} = \frac{0.00459}{8.38} = 0.000548 \text{ s (0.548 ms)}$$

and the number of pulses available during the dwell is

$$N_p = \frac{T_d}{T_r} = \frac{0.000548}{10 \times 10^{-6}} = 55 \text{ (17.4 dB)}$$

The range of initial detection is

$$R_i = \frac{4}{3} R_d = \frac{4 \times 10,000}{3} = 13737$$

Expressed in decibels, the fourth power of this range is 165.0 dB.

Table 2. Example of Verification of Energy-to-Noise Ratio

Parameter	dB
P_t	67.0
δ_t	−67.0
G_t	41.4
σ_t	−20.0
A_r	0.0
N_p	17.4
L	−10.0
$(4\pi)^2$	−22.0
R_i^4	−165.0
η	174.0
F	−3.0
ENR	12.8

The previously derived parameters may be inserted into the original range equation to verify ENR at an initial detection range. Table 2 shows this calculation.

The ENR obtained is very close to the required 13.0 dB. The discrepancy is in rounding errors. Essentially, the major radar parameters have been established and the preliminary design is complete.

Admittedly, the foregoing exercise is idealized. In practice, several iterations would be required to firm the design.

Doppler Shift

Modern radar takes advantage of Doppler shift to separate moving targets and stationary clutter. This phenomenon manifests itself as an increase in the carrier frequency received from an incoming, moving target relative to the frequency of transmission. The magnitude of the Doppler shift is given by

$$\Delta F = \frac{2V_t F_r}{c}$$

where V_t is the radial component of target velocity, F_r is the radar frequency, and c is the velocity of propagation.

The impact of Doppler shift on radar design is illustrated best by example. Suppose that it is required to detect targets having incoming velocities ranging from 100 to 1000 m/s.

For the first case, assume that the assigned radar frequency is in the L-band at $F_r = 1.0$ GHz. The minimum Doppler shift is

$$\Delta F_{\min} = \frac{2 \times 100 \times 10^9}{3.0 \times 10^8} = 667 \text{ Hz}$$

and the maximum is

$$\Delta F_{\max} = \frac{2 \times 1000 \times 10^9}{3.0 \times 10^8} = 6667 \text{ Hz}$$

Suppose further that a clutter canceler such as MTD is employed. One characteristic of these cancelers is that their frequency response function repeats at intervals of the pulse repetition frequency (PRF). That is, nulls will appear at zero frequency and at integral multiples of the PRF. In this case, it seems reasonable to center the expected target spectrum between nulls. This would require that

$$\text{PRF} = 6667 + 667 = 7334 \text{ Hz}$$

The corresponding pulse repetition interval (PRI) is 136.4 μs. The two-way time delay to and from a target at range, R, is given by

$$\tau = 2R/c$$

Therefore, the first blind range occurs at

$$R = \frac{c \cdot \text{PRI}}{2} = \frac{3 \times 10^8 \times 136.4 \times 10^{-6}}{2} = 20.5 \text{ km}$$

A crucial factor in MTI design is the fraction, p, of PRF for which an adequate response is required. In this case, that fraction is given by

$$p = \frac{6667 - 667}{7334} = 0.82$$

This response is easily obtained using appropriate feedback and feedforward coefficients in a two-stage canceler. Thus, the design appears sound.

Now, consider the effect of increasing the transmission frequency. Suppose the radar is to operate in K_a band at $F_r = 35$ GHz. In this case, the minimum target Doppler is

$$\Delta F_{\min} = \frac{2 \times 100 \times 35 \times 10^9}{3.0 \times 10^8} = 23,333 \text{ Hz}$$

and the maximum is

$$\Delta F_{\max} = \frac{2 \times 1000 \times 35 \times 10^9}{3.0 \times 10^8} = 233,333 \text{ Hz}$$

If a PRF of 7334 were used here, there would be 32 blind velocity zones across the target spectrum. This is probably unacceptable. If a PRF were selected to center the target spectrum, its value would be

$$\text{PRF} = 233,333 + 23,333 = 256,666 \text{ Hz}$$

The corresponding PRI is 3.9 μs with blind ranges occurring at a spacing of 585 m. Again, this value is probably unacceptable. Obviously, a compromise is warranted but, whatever the PRF choice, there will remain a large number of both blind velocity zones and blind range zones.

This example shows the difficulty of designing at a high radar frequency.

Coherency

Effective utilization of the Doppler shift requires that the transmission and local oscillators bear a constant time-invariant, phase relation. This is termed *coherency*. An example best illustrates its importance.

The carrier signal during a given transmission may be represented by

$$f_{t1} = \cos(\omega_1 t + \phi_1)$$

where ω_1 is the radian frequency of transmission and ϕ_1 is an arbitrary phase term. The return from a clutter scatterer located at a time delay τ is given by

$$f_{r1} = \cos[\omega_1(t - \tau) + \phi_1]$$

In the noncoherent case, the local oscillator signal used to convert the return to video may be written as

$$I_{\text{lo}} = \cos \omega_2 t$$

There are a number of procedures for processing the video output. A preferred approach is to utilize a quadrature local oscillator given by

$$Q_{\text{lo}} = \sin \omega_2 t$$

It is assumed that the two local oscillators are free-running at a constant frequency. During transmission of the second pulse, assume that the transmission has changed frequency and phase. Its form is now

$$f_{\text{t2}} = \cos(\omega_3 t + \phi_3)$$

In the simplest of clutter cancelers, the two samples in each channel are subtracted and a magnitude formed as the square root of the sum of the squares. Simple trigonometric manipulation shows that the output magnitude has the following form.

$$M = \{2 - 2\cos[\phi_1 - \phi_3 + (\omega_3 - \omega_1)\tau + (\omega_2 - \omega_3)T]\}^{1/2}$$

In the case where all signals are coherent, all frequencies and phases are equal, the argument of the cosine function is zero and the output magnitude is zero as desired. However, when coherency is not maintained, that argument may range anywhere from zero to 2π. In the worst case, it will be π. Then, the output will be twice the input level and clutter will have been amplified rather than canceled. Clearly, coherency is mandatory if clutter is to be rejected.

Signal Synthesis

To maintain coherency, it is usual to design the frequency synthesizer based on frequency multiplication of crystal controlled oscillators and offset modulation of these signals. There are numerous techniques for achieving coherency. As an example, one technique is depicted in Fig. 2. This example shows a typical interface between the signal synthesizer and the microwave and intermediate frequency receivers.

Based on this block diagram example, an example of the methodology used to select synthesizer parameters is presented. For this example, it is assumed that the system is to operate at 10,000 MHz.

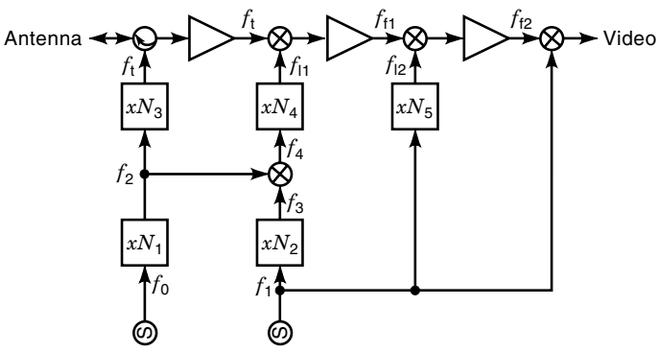

Figure 2. Signal flow diagram using typical frequency synthesizer and radar receiver. Coherent reception is ensured by careful selection of local oscillator and intermediate frequencies.

The first decision is the selection of oscillator frequency, f_1. This signal will serve as the *system clock*. Among other functions, it will provide timing for pulse width and pulse repetition interval events. Obviously, its selection also sets the second intermediate frequency (IF) so that final frequency conversion is to direct current or video. A good choice is f_1 = 100 MHz. The period of this signal is 10 ns, which allows for timing events in integral multiples of this period. It is also a good choice for the second IF where filtering must be provided to pass only the received pulse spectrum while rejecting interference outside that spectrum. Filter design is relatively straightforward when the required bandwidth is, roughly, one-tenth of the center frequency. Thus, the selected IF will support a pulse spectrum of 10 MHz which corresponds to a pulse width of 100 ns.

The next selection is that of the first IF. The transmission frequency is

$$f_{\text{t}} = N_1 N_3 f_0$$

and, assuming that the sum frequency is taken at the offset modulator output, the first local oscillator signal is

$$f_{\text{l1}} = (N_1 f_0 + N_2 f_1) N_4 = N_1 N_4 f_0 + N_2 N_4 f_1$$

Assuming that the local oscillator (LO) frequency is higher than the transmission frequency, the first mixer output or first IF is given by

$$f_{\text{f1}} = f_{\text{l1}} - f_{\text{t}} = N_1(N_4 - N_3) f_0 + N_2 N_4 f_1$$

The oscillator f_0 is varied to provide tuning of the transmission frequency. Therefore, it must not be allowed to vary the first IF. This dictates that $N_4 = N_3$ and the resultant first IF is

$$f_{\text{f1}} = N_2 N_4 f_1$$

It is always good design practice to avoid image responses in the first IF. When the first LO is spaced by the IF above the transmission, it will transfer the transmission to the IF. However, it will transfer also any signal spaced by the IF above the LO back to IF. The latter is termed an *image response*. Normally, the microwave receiver provides filtering to pass only those RF channels assigned to that system and to attenuate other signals outside that band. In the example, suppose that the allocated band ranges from 10,000 MHz to 11,000 MHz. Then, if an IF of 500 MHz was chosen and the target frequency was 10,000 MHz, the image would lie at 11,000 MHz within the receiver passband. A higher IF would force the image down the slope of the receiver filter and provide some image attenuation. Thus, it is reasonable to require the first IF to be at least one-half of the allocated system bandwidth. Even higher values are encouraged to provide more image attenuation.

In the example, it is seen that the first IF must be an integral multiple of 100 MHz. Furthermore, that integer must be factorable into two smaller integers. This means that a value of 700 MHz is not allowable because 7 is a prime integer. Similarly, 1100 and 1300 MHz are disallowed. A reasonable choice is 1500 MHz. Then, the multiplication integers might be chosen as $N_2 = 3$ and $N_3 = N_4 = 5$.

The next choice is the selection of frequency for the other basic oscillator, f_0. By requirement, it must follow that

$$N_1 N_3 f_0 = 10{,}000$$

However, since $N_3 = 5$ has been chosen, the requirement reduces to

$$N_1 f_0 = 2000$$

Here, a good choice might be $f_0 = 200$ MHz. This would require $N_1 = 10$ which decomposes nicely into 5×2. From an implementation standpoint, smaller integer multipliers are to be preferred.

The final selection is the second LO. The only choices are 1400 and 1600 MHz. The former requires $N_5 = 7 \times 2$, whereas the latter requires $N_5 = 4 \times 4$. Clearly, the better choice is $f_{l2} = 1600$ MHz.

Frequency multiplication is achieved by applying a given signal to a nonlinear device. This device produces harmonics of the input frequency. Subsequent filtering removes the undesired harmonics with the residual being the multiplied frequency. The simplest case is the frequency doubler. Here, the nonlinear characteristic is $y = x^2$. Assume that the input signal is given by

$$x = \cos[\omega_1 t + \phi(t)]$$

where ω_1 is the input radian frequency and ϕ is a time varying noise process. Then, the output signal is

$$y = \tfrac{1}{2}\{\cos[2\omega_1 t + 2\phi(t)] + 1\}$$

Thus, the output frequency is twice that of the input. However, note that the noise function has been doubled also. It is a characteristic of frequency multipliers that frequency modulated noise will be multiplied also by the multiplication factor. This disadvantage is offset by the basic coherency afforded by these devices.

By simple signal tracing, the reader may verify that the various frequencies produced in the given multiplication and heterodyning processes are reduced to direct current at the video output. By analogy, all noise processes are canceled by the time they reach video. This is the case only because no time delays were postulated in any of the circuit paths. In particular, the time delay to and from a clutter scatterer was ignored. In reality, the FM noise associated with oscillator f_0 and reflected from clutter will not be canceled totally and will appear at the video output. This noise is of serious concern to the designer and its level at the source must be controlled carefully.

Power Amplifier

Once the system designer has chosen average power, pulse width, and peak power, little else is required for the power amplifier element. The remainder of the design becomes a circuit design problem. However, the designer must be aware that this element represents the best candidate for cost effectiveness. Power amplifiers and their attendant modulators and power supplies are expensive, large, and heavy. High-power amplifiers are highly expensive, very large, and very heavy. Moreover, they represent a hazard to operating personnel owing to the high voltages involved and the high radiation levels required. Failure rates are often high due to the large component stress induced by generated heat within internal circuitry. Finally, periodic maintenance is complicated by the weight of components and the fact that most components must be submerged in heat-dissipating liquids. All of these disadvantages are balanced only by the single gain factor offered by this element.

In making system level trade-offs, the careful designer is advised to select the largest antenna possible to reduce the requirements on the power amplifier. With the possible exception of exotic phased arrays, antennas are, generally, less expensive, more reliable, less hazardous, and more maintainable than their power amplifier counterparts. In addition, the larger antenna offers narrower beamwidths and increased angular accuracy.

Power output notwithstanding, radar frequency bandwidth may be an important design consideration. The first requirement is the ability to pass, with high fidelity, a narrow pulse spectrum. Pulse widths on the order of 100 ns having bandwidths of 10 MHz are not uncommon. The klystron vacuum tube provides an instantaneous bandwidth capable of supporting most pulse applications. However, when rapidly tuned frequency agility is required, amplifier bandwidth becomes very critical. In applications designed to thwart narrowband spot jamming, agility bandwidths on the order of 1000 MHz may be required. Tuning intervals of only a few milliseconds may be dictated. These parameters are supported easily by the frequency synthesizer, but, for example, a mechanically tuned klystron will not meet the tuning speed desired. In that case, wideband devices such as the traveling wave tube (TWT) must be used.

A potentially serious problem arises when broadband power amplifiers are utilized. This is radiation of broadband noise. The amplifier not only provides gain to the transmission signal but to thermal noise as well. When this energy impinges another friendly radar in the vicinity, the noise can cause sensitivity degradation in the victim radar. Selectivity in the victim radar can be used to reject the signal spectrum of the interference but will not reject the broadband noise. Table 3 depicts a typical scenario.

In the table, η is the inherent noise power density at the power amplifier input, G_a is the amplifier gain, F is its noise figure, G_t is transmit antenna gain, R is a typical separation between interferer and victim, A_r is the victim antenna capture area, G_{sl} is a typical victim sidelobe rejection, and P_r is the resultant noise density at the victim receiver. Suppose that the victim receiver noise figure is 3 dB. Then, the re-

Table 3. Computation of Received Noise in a Typical Interference Scenario

Parameter	Value	Units
η	-174	dB/mW · Hz^{-1}
G_a	60	dB
F	20	dB
G_t	40	dB
4π	-11	dB
R^2	-66	dB/m^2
A_r	0	dB/m^2
G_{sl}	-20	dB
P_r	-151	dB/mW · Hz^{-1}

ceiver noise density in the absence of interference is $-174 + 3 = -171$ dB/mW · Hz. Thus, the interference causes a 20 dB sensitivity degradation each time the main beam of the interferer passes the victim.

This unacceptable situation may be alleviated by reducing the amplifier gain and, consequently, its output power. However, that would require an increase in antenna gain with no overall benefit. Reduction of the victim sidelobe level would help but that antenna may not be within the purvey of the designer of the interfering radar. The ultimate solution might be in incorporating a low-noise high-gain, preamplifier to drive the main power amplifier. This has the potential for reducing the noise output by 17 dB but the problem remains. Scenarios of this type require careful consideration.

Antenna

Once the basic antenna area has been selected based on power-aperture product requirements, the designer is free to choose the horizontal and vertical dimensions. Longer dimensions produce narrower beamwidths in that plane. Thus, the antenna might be long horizontally and short vertically. This would produce a fan beam narrow in azimuth and broad in elevation. However, certain applications might require a rotated fan beam with narrow elevation and wide azimuth beamwidths. In some cases, a square or circular aperture might be selected to give comparable beamwidths in both planes. In all cases, the antenna gain should be constant to satisfy range equation requirements.

The antenna radiation pattern is, by reciprocity, identical to the reception pattern. The far-field electrical field intensity in a given plane, analogous to voltage in an electronic circuit, is determined by taking the Fourier transform of the current distribution across the antenna face in that dimension. Thus,

$$E(\phi) = \int_{-a/2}^{a/2} A(z) \exp\left(j2\pi \frac{z}{\lambda} \sin\phi\right) dz$$

where ϕ is the angle off boresight, a is the linear dimension of the antenna, $A(z)$ is the current distribution, and λ is the wavelength. When the current distribution is constant or uniform, the gain is maximized and the normalized pattern is given by

$$E(\phi) = \frac{\sin[\pi(a/\lambda)\sin\phi]}{\pi(a/\lambda)\sin\phi}$$

The power gain, in decibels, is

$$G_t = 20 \log E(\phi)$$

This pattern is plotted in Fig. 3 for the case where $a = 1.0$ m and $\lambda = 0.03$ m.

Sidelobe levels may be depressed by weighting the distribution as a function of length. An example is the cosine function for which

$$A(z) = \cos\frac{\pi z}{a}$$

The corresponding normalized intensity pattern is

$$E(\phi) = \frac{\pi}{4}\left[\frac{\sin(\psi + \pi/2)}{\psi + \pi/2} + \frac{\sin(\psi - \pi/2)}{\psi - \pi/2}\right]$$

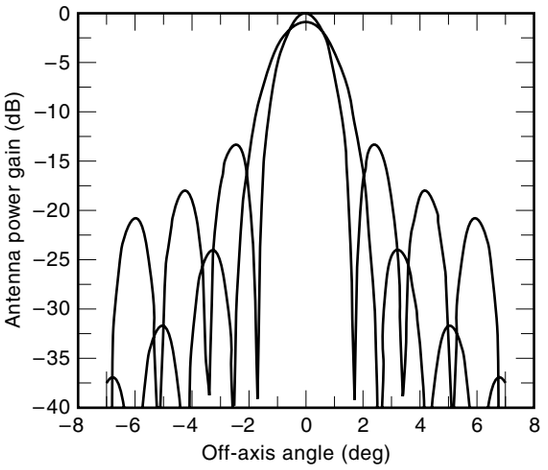

Figure 3. Comparison of antenna patterns using uniform and cosine aperture illumination. A cosine illumination gives a significant reduction in unwanted sidelobes.

where $\psi = \pi(a/\lambda) \sin \phi$. In this case, the aperture is not illuminated fully and the main beam gain is reduced to 0.81 (-0.9 dB) relative to the uniformly illuminated case. This pattern is shown in Fig. 3 also.

The uniform distribution yields a first sidelobe level of 13 dB relative to mainlobe gain while the cosine distribution gives a 23 dB first sidelobe. The respective beamwidths are 1.53° and 2.07°.

Skolnik (2) has a definitive dissertation on antenna design.

Microwave Receiver

The most important parameter associated with the microwave receiver is the *noise figure.* That parameter sets the basic sensitivity of the radar. The noise figure of any electronic device is defined as the ratio of input SNR to output SNR. It is a measure of the contribution of that device to overall system noise level.

If the first component in the receiver chain is the mixer used to convert to first IF, then the loss in that mixer dictates the noise figure. This loss could be as high as 10 dB even for a well-designed mixer. If this noise figure is unacceptably high, it may be reduced by incorporating a low noise radar frequency amplifier ahead of the first mixer. The noise figure of the combined amplifier-mixer is given by

$$F_0 = F_1 + \frac{F_2 - 1}{G_1}$$

where F_1 is the noise figure of the amplifier, F_2 is the mixer noise figure, and G_1 is the amplifier gain. In a typical design, F_1 might be a factor of two (3 dB) and the gain might be a factor of 100 (20 dB). Then,

$$F_0 = 2 + \frac{10 - 1}{100} = 2.09\ (3.2\ \text{dB})$$

This improvement of almost 7 dB equates to a reduction in required transmission power or antenna aperture of approximately a factor five.

A second important feature of the microwave receiver is component protection from the high power level of the transmission. Often, this protection is provided by a circulator. Figure 4 shows a schematic representation of this device.

The circulator may be viewed as a circular racetrack where the line length between the transmitter port and the receiver port is one-quarter wavelength, the length between transmitter port and antenna port is also one-quarter wavelength and that between antenna port and receiver port is one-half wavelength. At the transmitter port, the signal is divided with one-half traveling one-quarter wavelength counter-clockwise to the receiver port and one-half traveling three-quarter wavelengths clockwise to the receiver. Thus, the two signals arrive out of phase at the receiver port and cancel. On the other hand, the received signal at the antenna port is divided also but, on both the counter-clockwise and clockwise paths, the signals traverse the same one-half wavelength. Thus, they arrive in-phase and recombine to preserve the target return.

Theoretically, the transmission will be canceled exactly with no residue left at the receiver input. However, the circulator line lengths can be designed only for one particular frequency. When the radar must operate over a band of frequencies, the line lengths may not match the actual frequency. The result is imperfect cancellation. Circuit tolerances may also alter line lengths. For these reasons, only isolation on the order of 20 dB can be guaranteed.

A final function provided by the microwave receiver is *frequency selectivity.* The receiver need pass only the pulse spectra of transmissions within it's allocated operating band. Signals received from radars operating outside this band should be rejected to avoid potential interference. When the radar frequency is much higher than that of expected interferers, then the natural cut-off frequency of wave guide may provide adequate selectivity. However, in most cases, special filtering circuitry must be employed.

This problem is compounded further by the fact that the pulse emission spectral width essentially, is, infinite. The spectral density is given by

$$H(f) = \left[\frac{\sin(\pi f \tau)}{\pi f \tau}\right]^2$$

where f is the frequency away from the carrier and τ is the pulse width. The envelope of the spectrum is (in decibels),

$$H_e(f) = -20\log(\pi f \tau)$$

Suppose that the frequency separation between victim and interferer is 5 GHz and the interference pulse width is 200 ns. Then, the spectral attenuation at the victim frequency is

$$L_s = -20\log(\pi \times 5 \times 10^9 \times 200 \times 10^{-9}) = -70 \text{ dB}$$

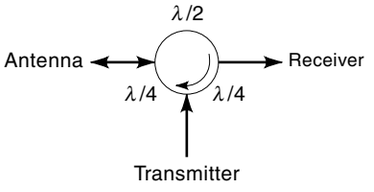

Figure 4. Circuit schematic of a circulator used for receiver protection. The circulator utilizes path length differences to cancel the transmission of the receiver port.

Table 4. Computation of Received Power Level in a Typical Interference Scenario

Parameter	Value	Units
P_t	70	dB/mW
G_t	40	dB
4π	−11	dB
R^2	−86	dB/m^2
A_r	0	dB/m^2
G_{sl}	−20	dB
L_s	−70	dB
P_i	−77	dB/mW

A typical interference scenario is depicted in Table 4 where the applicable range equation is tabulated.

In the table, P_t is the assumed interferer peak power level (10 kW), G_t is its antenna gain, R is the range separation (20 km), A_r is the victim capture area, G_{sl} is the victim maximum sidelobe level, L_s is the spectral attenuation, and P_i is the resultant interference level received by the victim radar. Assume that the noise figure of the victim radar is 3 dB and that its ultimate processing bandwidth is 5 MHz. Then, the victim receiver noise level is

$$P_v = -174 + 67 + 3 = -104 \text{ dB/mW}$$

Thus, the interference SNR is 27 dB, which guarantees unwanted interference detection in the victim radar.

Intermediate Frequency Receiver

Attributes of the IF receiver that are of concern to the system designer are overall gain, IF filtering, video filtering, and digital converter saturation protection.

The receiver must provide sufficient gain to place minimum signals and noise within the digital converter range. Typically, the receiver noise is set at about 2 mV at the converter input. Assuming a load of 50 Ω, this represents a power level of −41 dB/mW. The receiver input noise level is dependent on receiver bandwidth and noise figure. Assume a bandwidth of 5 MHz and a noise figure of 3 dB. Then, the input noise level is −104 dB/mW. The required gain is then 63 dB. This is a net figure and must account for losses in frequency conversion and filtering.

Usually, IF filtering is provided to ensure the passage of the return pulse with adequate fidelity but to reject unwanted interference signals. Fidelity will require an IF bandwidth on the order of ten times that of the received pulses. Thus, a pulse width of 1 μs might require an IF bandwidth of 10 MHz. The objective is to provide only sufficient filtering to reject interference but to not compromise the design of the matched filter at video.

A very important component of the receiver design is the filter that immediately precedes the digital converter. Commonly this is referred to as the *matched filter.* Here, an attempt is made to maximize the SNR available at the instant when the pulsed return is sampled. Choices for the architecture of this filter are limitless. The simplest case is the first-

order low-pass filter. In the Laplace transform domain, this filter has a transfer function given by

$$H(s) = \frac{\omega_c}{s + \omega_c}$$

where ω_c is a radian corner frequency defining the filter bandwidth. The magnitude squared response of this filter is

$$H(f) = \frac{f_c^2}{f^2 + f_c^2}$$

where $\omega_c = 2\pi f_c$ and f is the frequency variable. The noise equivalent bandwidth of this filter is

$$B_{eq} = \frac{1}{2}\int_{-\infty}^{\infty} \frac{f_c^2}{f^2 + f_c^2} df = \frac{\pi f_c}{2}$$

For a rectangular input pulse of width τ, the peak response occurs at $t = \tau$ and is given by

$$V_{max} = 1 - \exp(-2\pi f_c \tau)$$

At the peak, the SNR is

$$\text{SNR} = \frac{[1 - \exp(-2\pi f_c \tau)]^2}{\eta(\pi f_c/2)}$$

where η is the receiver noise power density. A plot of this function will show that its maximum occurs when $f_c\tau = 0.2$. Matched filter theory states that the maximum SNR attainable is equal to twice the ratio of pulse energy to noise power density. That is,

$$S_{max} = 2\tau/\eta$$

In this case, the ratio of optimized SNR to maximum achievable may be shown to be -0.9 dB. This loss may be reduced by using higher order filters at the expense of increased circuit complexity. Schwartz (3) derives the matched filter theorem and gives detailed examples.

It is imperative to ensure that input signals do not exceed the dynamic range of the digital converter. Excess signals will not be decoded properly and the output data may cause interference. It is usual to provide converter protection by implementing a limiter in the final IF stage. The limit level is set somewhat below the actual converter peak capability to account for receiver gain fluctuations. This offset, effectively, reduces receiver dynamic range. In advanced designs, level sensors and feedback may be used to adjust receiver gain so that the limit level may be set very close to the peak of the converter range.

The limiting should not be applied at video. The nonlinearity of the limiter creates harmonics of the input signal. If that signal is clutter, these harmonics will not be canceled in the MTD and undue interference will result.

Waveform

The term *waveform* refers to the pulse width and pulse repetition frequency (PRF) of the transmitted signal. However, other characteristics such as frequency, phase, and amplitude modulations may be included in its definition.

Generally, pulse width is selected to yield the required range measurement accuracy. However, a longer pulse may be required to achieve the energy necessary for reliable detectability. Pulse widths ranging from a few tens of nanoseconds to a few microseconds are not uncommon.

In those cases where available peak power is limited, it may be advisable to incorporate *pulse compression.* In this technique, modulations are applied to a relatively long pulse on transmission. Appropriate circuitry within the receiver decodes these modulations to produce a narrow pulse. The most common modulation is binary phase coding. This consists of applying either a zero or 180 deg phase shift to each subpulse within the longer pulse. Decoding is achieved by applying the received pulse to a series of delay lines spaced by multiples of the subpulse width. The output of each delay is multiplied by the inverse code and the outputs summed to produce the compressed pulse. The drawback to this technique is that it produces unwanted responses termed *time sidelobes* which are a source of potential interference and confusion. There exists a class, Barker codes, which yield alternating sidelobes of zero and unity while producing a compressed amplitude equal to the code length. These are in popular use but the maximum known length is 13.

Pulse repetition frequency may be used to classify a given radar into one of three categories. In a low PRF system, the pulse repetition interval (PRI) is chosen such that no range blinding occurs over expected target ranges. However, there may be blind velocities produced by the MTI. A high PRF design dictates no velocity blinding over expected target velocities but blind ranges may occur. A compromise waveform is medium PRF which has both range and velocity blinding. The choice of category is application specific, with no particular choice being universally superior. In practice, targets may be detected at extremely long range and may have very high velocity. Thus, pure low or high PRF systems, probably, do not exist. All waveforms may be viewed as medium PRF. The choice of waveform toward low or high PRF depends upon the acceptable number of blind range zones and blind velocity zones.

Total range and velocity blinding may be avoided by choosing a waveform set having multiple repetition frequencies. This multiplicity also allows for range and velocity ambiguity resolution. The PRF may be changed on a scan-to-scan basis or during each beam dwell. The disadvantage of the latter approach is that clutter transients may follow a PRF change and reduce the effectiveness of clutter cancellation. This may require receiver blanking during the clutter settling interval, which wastes valuable transmission energy and reduces detectability. Conversely, the former approach complicates ambiguity resolution because the target will probably change range between scans.

Range ambiguity resolution is illustrated best by assuming PRF transitions during a single beam dwell. In this case, it may be assumed that target range remains constant while both frequencies are processed. Let the repetition interval on the first PRF be T_1 and on the second be T_2. Assume that the measured time delay between transmit pulse and detected pulse is τ_1 on the first PRF and τ_2 on the second. These are the ambiguous range measurements. Assume that the unknown unambiguous time delay is T. That value must satisfy both of the following equalities.

$$T = \tau_1 + N_1 T_1$$
$$T = \tau_2 + N_2 T_2$$

Usually, determination of the two integers, N_1 and N_2, is accomplished by iteration or trial and error. Either integer may be used to compute true range.

Because the combined pattern of two frequencies will repeat at some long range, the resolution procedure, in reality, only resolves the ambiguity to within some other ambiguity. The pattern repeats, in general, at the product of the two repetition intervals when those intervals are expressed as integral multiples of the sampling interval unless there are common factors involved. As an example, assume that $T_1 = 29.0$ microseconds (μs) and that $T_2 = 37.0$ μs. Furthermore assume a sampling interval of $T_s = 0.2$ μs. Then $T_1 = 145$ T_s and $T_2 = 185$ T_s. The product is $P = 145 \times 185 \times 0.2 = 5365$ μs. However, the common factor of five reduces the pattern repetition to 1073 μs (161 km). A better choice might be $T_1 = 29.8$ μs and $T_2 = 36.2$ μs. Then, the product is $P = 149 \times 181 \times 0.2 = 5393.8$ μs (809 km) and, since the integers are prime, that is the maximum resolved ambiguity.

Dynamic Range

The ratio of maximum to minimum signal levels that may be processed linearly without concern for harmonic production or small signal suppression is termed the *dynamic range* of the system. This parameter is set either by the characteristics of the microwave and IF amplifiers or those of the analog-to-digital converter (ADC).

For low-level input signals, electronic amplifiers are linear and the output level is proportional to the input level. However, as the input level increases, the output begins to approach a constant independent of input level. This condition is termed saturation. When a high-level clutter signal and a low-level target signal are processed simultaneously through a saturated amplifier, the target signal is suppressed. Although the receiver noise is suppressed also, the FM noise carried by clutter is not affected. The overall result is a decrease in target SNR.

The ADC usually determines the system dynamic range. The theoretical noise level due to quantization in the ADC is $\frac{1}{12}$ of one least significant bit (LSB). This is equivalent to a power level of -11 dB relative to the LSB. However, practical ADC devices exhibit noise levels well above theoretical. Typically, a noise level of -1 dB can be expected. The maximum signal that may be processed linearly is dependent upon the number of bits available at the ADC output. Consider a 12-bit device. Because one bit must be assigned to the sign of the output, the maximum peak signal is 20 log $(2^{11}) = 66$ dB. The corresponding rms level is 63 dB. Thus, the apparent dynamic range is 64 dB.

The ADC noise will add to the input receiver noise and reduce sensitivity. This reduction may be minimized by setting the receiver noise somewhat higher than that of the ADC. For example, a receiver noise level 6 dB above ADC noise yields a 1 dB degradation. Now, the dynamic range is reduced to 58 dB.

Compounding the problem are fluctuations in receiver gain over ambient temperature. Should that gain drift downward by 6 dB, the sensitivity degradation would be 3 dB. This unwanted circumstance is avoided by elevating the nominal receiver noise level an additional 6 dB. If the gain should increase by 6 dB and if the IF limit level were set exactly at the maximum ADC level, then the higher level would overload the converter. This is avoided by setting the limit level 6 dB below that of the ADC. The overall result of these adjustments is a 12 dB decrease in dynamic range to a value of 46 dB.

Additional dynamic range may be obtained by increasing the number of bits available from the ADC. Each added bit represents an increase of 6 dB in the dynamic range. However, adding bits reduces processing speed. Currently, devices are available that output 14 bits at rates of 10 MHz. In the near future, it is expected that 16 bits or more may be achieved at rates up to 30 MHz or higher.

It is possible to monitor receiver noise level and, using feedback, to control the receiver gain. This would enable the receiver noise and IF limit level to be maintained constant relative to the ADC parameters. The result would be a 12 dB increase in dynamic range. Use of this technique with a 14 bit ADC enables a dynamic range of 70 dB.

Target Detection

A primary function of the search radar is to provide detection of targets. Usually, this is achieved by comparing received signals to a preset threshold. For this function, the operative measure of performance is probability of detection. This probability depends upon input SNR and allowable false alarm rates.

Detection theory is couched in Rician statistics. This theory treats the problem of the probability that the magnitude of a sinusoidal signal imbedded in Gausian noise will exceed a given threshold. [See Schwartz (4) for a detailed derivation.]

The correct threshold is determined by electing an allowable probability of false alarm, μ. That probability is given by

$$\mu = \exp(-V_t^2/2\sigma^2)$$

where V_t is the threshold voltage and σ is the root mean square (rms) noise voltage. It is usual to set this threshold based on a measured value of the average noise magnitude. That average is

$$m_1 = \sigma\sqrt{\frac{\pi}{2}}$$

The threshold is set at a constant, k, times the measured average. The proper selection of the constant is

$$k = \left[-\frac{4}{\pi}\ln\mu\right]^{1/2}$$

The threshold is related to the rms noise level and probability of false alarm as

$$V_t = \left[\frac{-\ln\mu}{2\sigma^2}\right]^{1/2} = \left[\frac{-\ln\mu}{2}\right]^{1/2}$$

where the assumption that the rms noise level is unity does not result in loss of generality. Under that assumption, the probability of target detection is

$$P_d = 1 - \int_0^{V_t} q(r)\,dr$$

where

$$q(r) = \exp(-s^2) r \exp(-r^2/2) I_0(rs\sqrt{2})$$

Here, s^2 is the target SNR and I_0 is the modified Bessel function of the first kind and zero order. The integral cannot be evaluated in closed form. However, it is solved easily by numerical integration on a digital computer. This evaluation is aided by the following power series expansion of the modified Bessel function.

$$I_0(z) = \sum_{n=0}^{\infty} \frac{z^{2n}}{2^{2n}(n!)^2}$$

A typical application of this technique yields the curves shown in Fig. 5.

In the figure, it is noted that reliable detection requires an SNR in excess of approximately 13 dB. The penalty for reducing false alarm rate by one order of magnitude is about 1 dB in terms of required SNR.

Seldom is target detection based on the result due to a single received pulse. Rather, integration of some form is employed to reduce the SNR required on a single pulse. Pulse integration is possible since there are, generally, multiple returns available during a beam dwell.

Suppose that the antenna azimuth beamwidth is 2 deg, the scan rate is 60 RPM and the repetition interval is 30 μs. These parameters result in the availability of 185 target return pulses over the beam dwell. For simplicity, assume that these pulses are of equal magnitude. Furthermore assume that an allowable overall false alarm interval from the signal processor is 1 s and that the pulse width and attendant sampling interval is 0.2 μs. Then, the number of range cells is 150 and the allowable false alarm interval from each is 150 s.

The simplest integration technique is, essentially, to do nothing. Since there are 185 equally probable opportunities for detection, the overall probability of detection is

$$P_o = 1 - (1 - P_d)^{185}$$

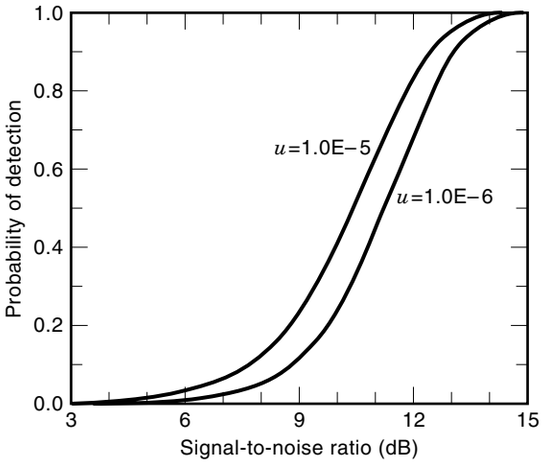

Figure 5. Detection performance as a function of signal-to-noise ratio. Curves represent two different false alarm rates. Probability of detection increases as SNR increases but decreases as false alarm rate is decreased.

where P_d is the single sample probability. Suppose that an overall detection probability of 0.9 is desired. Then, on a per-sample basis, the required probability is $P_d = 0.012$. The allowable probability of false alarm is the ratio of the repetition interval to the allowable false alarm interval. Thus,

$$\mu = \frac{30 \times 10^{-6}}{150.0} = 2.0 \times 10^{-7}$$

This combination of parameters results in a required, per-pulse SNR of 7.0 dB.

At the other extreme is completely coherent integration. In this case, voltages from all 185 pulses are added before comparison to a threshold. The result is an increase in SNR of 10 log 185 = 22.7 dB. On the other hand, the decision interval has been increased by a factor of 185 so that the allowable false alarm probability is now

$$\mu = \frac{185 \times 30 \times 10^{-6}}{150.0} = 3.7 \times 10^{-5}$$

At the corresponding threshold, the required integrated SNR for a 0.9 probability of detection is 12.1 dB. The per-pulse requirement is only -10.6 dB. Therefore, the improvement afforded by coherent integration is 17.6 dB. This is a very significant improvement, because it reduces the required power-aperture product by almost two orders of magnitude.

Truly coherent integration may be obtained only through the use of fairly sophisticated processes, such as the discrete Fourier transform discussed later. However, there are available simpler approaches that achieve notable improvements. One such technique is the binary, or Markov chain, integrator.

The binary integrator is implemented by assigning a digital counter to each range cell in ambiguous range space. If a given sample exceeds a preset threshold, the counter is incremented by one. If not, the counter is decremented. The counter is not allowed to go negative nor to exceed some positive value. A detection is declared when the counter achieves some predetermined threshold.

The design of a binary integrator is an interesting exercise. Counter threshold is the parameter subject to trade-off. The first step is determining the proper per-pulse threshold necessary to hold the overall false alarm interval to the allowable level. It may be shown (5) that the expected number of samples required to transition from a counter state of zero to a state of N is

$$E_{oN} = \frac{1}{p} \sum_{i=0}^{N-1} (N - i) \left(\frac{q}{p}\right)^i$$

where p is the per-pulse probability of false alarm and $q = 1 - p$. For a given counter threshold and allowable false alarm interval, it is straightforward to determine the required value of p and this sets the per-pulse threshold. The basic equation of the Markov chain is

$$P(m,n) = qP(m+1, n-1) + pP(m-1, n-1)$$

where p and q are now target detection probabilities on a per-pulse basis and $P(m,n)$ is the probability of being in state m after the nth step. The result is a set of equations that may be exercised iteratively to yield overall probability of detection, after a given number of received pulses, given per-pulse

probability. Iteration over input probability yields that value which achieves the required overall probability of detection. In the example, that value is 0.9. Finally, interpolation of tables of detection probability as a function of probability of false alarm and SNR yields a required SNR for the given overall probability as a function of the Markov threshold. An iteration over Markov threshold will show that there is an optimum threshold that minimizes required SNR while maintaining the desired false alarm rate.

Using the parameters of the current example, the described procedure was executed by computer simulation. The result shows that the optimum Markov threshold is 30 and, at that value, the required per-pulse SNR is −1.4 dB. This represents an improvement of 8.4 dB over the case having no integration. Although this remains 9.2 dB lower than the improvement afforded by coherent integration, it does represent a major improvement because it reduces the required power-aperture product by almost an order of magnitude.

Accurate threshold setting depends on an accurate measurement of the ambient noise level. Usually, this measurement is obtained by averaging the magnitudes of several range cells adjacent to a range cell under test. This average should slide as successive range cells are tested for detection. The variance of this measurement may be shown to be

$$V(N_a) = \frac{V(N_i)}{N}$$

where $V(N_i)$ is the variance of an individual noise cell and N is the number of samples averaged. Thus, the measurement error decreases as the number of samples increases. Typically, the number of samples used is on the order of 30 or more. It may be shown that the use of averaging contributes approximately 0.5 dB to the total processing loss. This loss is tolerable because averaging serves to maintain a constant average false alarm rate even when receiver gain fluctuates.

Target Measurement Accuracy

A primary function of the radar is to provide a measure of target location in either two- or three-dimensional space. Thus, the radar must measure target range and target bearing as a minimum. Additional measurements of elevation angle, velocity, and target cross section may be taken in advanced designs.

In the simplest design, range is determined by noting the time delay between transmitted pulse and received pulse. In this case, the accuracy can be no better than the pulse width. When improved accuracy is required, further processing of the received signals must be performed. One approach is to use a weighted average of successive range cells. The estimated range is computed as

$$r_e = \frac{M_1 r_1 + M_2 r_2}{M_1 + M_2}$$

where M_1 and M_2 are the magnitudes and r_1 and r_2 are the measured ranges in two adjacent range cells. This technique is referred to as *split gating*. The utility of this technique is based on the fact that the video filter output pulse is rounded rather than square so that pulse magnitude varies predictably with time delay.

The accuracy of any split gate technique depends upon pulse width and SNR. In general, the rms error is given by

$$\sigma_r = k_r \delta_r / \sqrt{S}$$

where k_r is a constant depending upon implementation parameters, δ_r is the pulse width measured in units of range, and S is the SNR. At higher SNR, the error may be reduced to a fraction of the pulse width. Note that in systems using pulse integration split gating may be used only if sums of pulse magnitudes are obtained or true coherent integration is employed. It is of no use with binary integration.

In simple applications, target bearing is determined by noting the angular orientation of the antenna at the time of detection. Thus, the accuracy can be no better than the azimuth beamwidth of the antenna. When improved accuracy is required, there are a number of beam splitting techniques available. A very sophisticated approach takes advantage of the known shape of the antenna pattern to form a curve fit of the received data. Solution of the resulting set of equations yields a very exact measure of azimuth. In all beam splitting techniques, the rms error will be given by

$$\sigma_a = k_a \theta_a / \sqrt{S}$$

where k_a is a constant related to antenna parameters and θ_a is the azimuth beamwidth. Higher values of SNR yield errors of a fraction of beamwidth. Skolnik (6) derived theoretical boundaries for measurement accuracy.

Except for some advanced designs where the antenna is scanned past the target in elevation as well as azimuth, elevation beam splitting is not possible. Therefore, the error remains the elevation beamwidth and this value may be quite large. This error can have a profound impact on scan-to-scan correlation algorithms.

In some applications, it is required that a measure of target cross section be obtained. This parameter might be used, for example, to distinguish bird and insect returns from aircraft. This measurement depends upon a priori knowledge of all the parameters comprising the radar range equation. Since these parameters may fluctuate, especially over time, the accuracy of this measurement probably is limited to ±3 dB.

Target Acquisition

In automatic systems, target acquisition is a requirement. Through this process, a target file is maintained for each detected target. This file contains a record of target range and bearing and, possibly, elevation, velocity, and cross section. Each file is updated after each antenna scan with the latest measurement data.

File updates are accomplished by performing scan-to-scan correlation. This process is effected by associating the latest detection data with earlier data using the concept of correlation windows. For each target, a window in space is established into which it may be expected that the next measured parameters from that target may fall. If a given set of parameters falls outside all established windows, then a new target is declared and a new file initiated. Correlation windows are, generally, rather large after initial detection but are allowed to decrease in size as the target history matures.

An example of the use of windows may be helpful. Assume a two-dimensional radar having a single elevation beam that

rotates at 60 RPM. Then, the data interval is 1 s. Suppose an initial target detection occurs at a range of 10,000 m and at a bearing of 0° (due north). Assume further that the maximum expected target velocity is 1000 m/s. Then, if the target is traveling tangentially, it could change bearing by 5.7°. If it travels radially, it could change range by ±1000 m. Thus, an appropriate correlation window might be ±6 deg in bearing by ±1000 m in range. Suppose, on the subsequent scan, that a target is reported at range of 9500 m and at bearing 0°. These parameters are well within the assumed correlation window and these data would be associated with the first detection. In this case, the apparent radial velocity is 500 m/s and the angular velocity is 0. It might be expected, therefore, that the third scan would reveal a target at 9000 m and 0° bearing. Then, the third scan correlation window could be reduced to zero width in both dimensions. In practice, that window must be increased to account for measurement error and possible target maneuver. However, its dimensions would remain much smaller than that for the second detection.

The concept of target file may be extended to target trajectory prediction. That prediction has a practical benefit in a variety of applications. For example, a ship defense radar might predict whether a given ballistic missile target will impact the ship or fall harmlessly into the sea. The latter determination would save the waste of one or more defensive weapon rounds. Another example is in airport surveillance where it is desirable to determine if two given targets are on a collision course. Trajectory prediction may be predicated on polynomial curve fitting. Its accuracy improves with the number of detections available and with the accuracy of the individual measurements.

A final application, in military designs, is *kill assessment.* Here, a rapid change in trajectory parameters may indicate weapon damage to the target and may indicate that engagement with further rounds is unnecessary. This ammunition saving is critical since the initial load is finite and there may be other threats following the first.

Clutter Rejection

It is mandatory that clutter rejection be given a high priority. Exceptions are those systems specifically designed to provide terrain mapping or weather detection. Clutter returns include backscatter from terrain, islands, the sea surface, and rainfall. In military applications, it also may be necessary to consider enemy dispensed chaff clouds. Except for wind driven rainfall and chaff, the clutter Doppler shift for a stationary radar is normally 0. However, its spectral width may be nonzero depending on local motion of the various scatterers.

In airborne applications, the clutter spectral bandwidth will be twice the platform velocity. This relatively wide band presents an interesting exercise in the design of clutter cancellation algorithms.

Clutter-to-noise ratio at the radar receiver is computed using the radar range equation except that clutter radar cross section is used instead of target cross section. Ideally, clutter levels would be calculated by performing a triple integral over the antenna pattern in two dimensions and over the return pulse shape in range. In practice, that integral is approximated. For surface reflections such as those from terrain and sea, the approximate clutter cross section is

$$\sigma_c = R\theta_a\delta_r\sigma_0$$

where R is clutter range, θ_a is azimuth beamwidth, δ_r is range cell width, and σ_0 is clutter cross section density. In a metric system, the dimensions of the latter parameter are square meters per square meter of surface area. For volume scattering from rain and chaff, the approximate cross section is

$$\sigma_c = R^2\theta_a\theta_e\delta_r\sigma_0$$

where θ_e is the elevation beamwidth and σ_0 is the clutter density in square meters per cubic meter of clutter volume.

Over the history of radar, there have been extensive efforts to measure and to model clutter cross section density. These efforts have resulted in a number of empirical models (7). The most precise of these is for rainfall. There, it is shown that the clutter density is proportional to the rainfall rate raised to a power of 1.6 and is proportional to the fourth power of radar frequency. For sea clutter, the models are less precise. However, the trend seems to indicate an increase with wave height, a linear increase with frequency, and a nonlinear increase with grazing angle. Terrain clutter is the least well defined because there are wide fluctuations in terrain type, local ground slope, type and depth of vegetation, presence of manmade structures, and soil composition. Lacking definitive models, the designer must be content with ensuring that all clutter levels within the dynamic range of the system are rejected to an acceptable level.

In modern, digital search radar, the most common defense against clutter is the use of MTD. These also may be referred to as clutter cancelers. In essence, these devices subtract the value of one received signal from that received one pulse repetition interval earlier. Since clutter has a zero-frequency Doppler shift, its value is 0 at the canceler output. A Doppler-shifted target return, depending on phasing, may be enhanced at the output. When both feed-forward and feedback are employed, the MTD may be viewed as a digital filter. A block diagram of a single stage MTD is given in Fig. 6. A general treatment may be found in Skolnik (8).

In this example, one feed-forward coefficient, A_1, and one feedback coefficient, B_1, are used. The term, $1/z$, is the z-transform representation of a delay of one repetition interval.

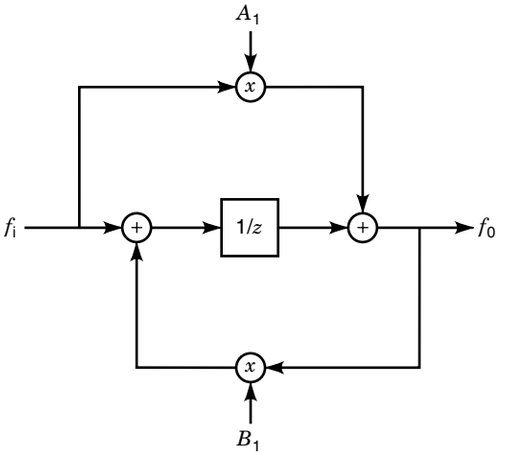

Figure 6. Single stage moving target indicator using both feed-forward and feedback. Frequency response may be shaped by varying the multiplier coefficients.

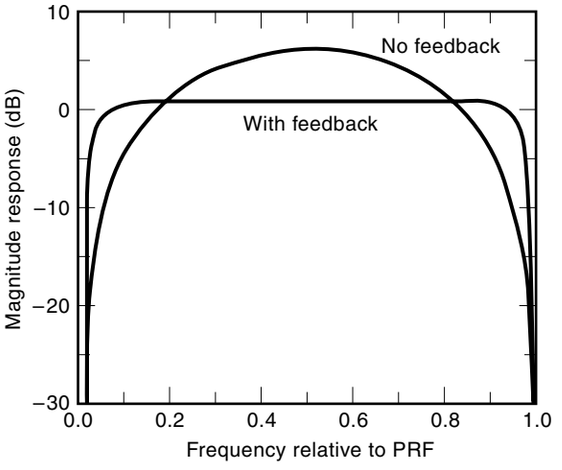

Figure 7. Frequency response of a single stage moving target indicator with and without feedback. Note the widening of the response when feedback is used.

A difference equation may be derived for this filter relating output to input. That equation is

$$f_o(n) = f_i(n-1) + B_1 f_o(n-1) + A_1 f_i(n)$$

Note that, when $A_1 = -1$ and $B_1 = 0$, the filter reduces to a simple subtractor.

To avoid blind phases, it is usual to implement identical MTI filters in the in-phase and quadrature channels of the radar Signal Processor. The output magnitude is taken as the square root of the sum of the squares of the two channels. The frequency response of the filter is obtained by plotting the steady-state output magnitude as a function of input signal Doppler shift. Typical results are given in Fig. 7.

In Fig. 7, the curve labeled "no feedback" represents the response for the simple subtractor. Its maximum response, 6 dB, occurs for a frequency equal to one-half PRF. However, at low frequencies, the response is poor. At 10% of PRF, a loss of almost 5 dB is incurred. This wide fluctuation is controlled using feedback. The curve marked "with feedback" shows the response for $A_1 = -1.0$ and $B_1 = 0.81$. In this case, the response is relatively flat at about 0.5 dB over 80% of the PRF. This response may be improved further by adding more delay lines and coefficients. Adjustment of pole and zero locations in the z-domain transfer function of higher ordered filters is helpful in tailoring the response to specific requirements. Filter designs using four delays and six coefficients are not uncommon.

In addition to clutter itself, clutter-carried FM noise can cause serious sensitivity degradation if it is not carefully controlled. The FM noise spectrum is generally wideband with significant levels extending for several megahertz. The total noise at the digital converter input is the integral of the product of the FM noise spectrum and the transfer function of the video filter. This total FM noise must be specified small compared to the total receiver noise level. As an example, assume that the digital converter dynamic range is 60 dB and that the video filter noise equivalent bandwidth is 1.0 MHz. To maintain the degradation due to FM noise at less than 1 dB, it would be necessary to require the total FM noise to be 66 dB below the clutter carrier. If the noise spectrum were flat, this would translate to a requirement that the noise density, as measured in a 1 Hz bandwidth, be 126 dB below the carrier.

Electronic Countermeasures

In military applications, the use of electronic countermeasures (ECM) by the enemy is, practically, a given condition. A prevalent form of ECM is broadband noise jamming. If the enemy can muster sufficient power levels and place this noise sufficiently close to the victim radar, then it can always defeat any radar. In those cases, the radar designer can do little to prevent degradation directly. However, there are scenarios in which jammer identification and/or frequency agility may be used to mitigate this degradation.

The total noise power received from a jammer is given by

$$P_r = \frac{P_j G_j B_r A_r G_{sl}}{4\pi R_j^2}$$

where P_j is the jammer noise power density, G_j is the jammer antenna gain in the direction of the victim radar, B_r is the radar receiver noise equivalent bandwidth, A_r is the radar antenna capture area, G_{sl} is the sidelobe antenna gain in the direction of the jammer, and R_j is the jammer range.

If the existence of jamming can be determined and the bearing angle of its source measured, then various weapons, such as home-on-jam missiles, can be brought to bear to destroy the jamming source. This may or may not be in time to prevent the ingress of hostile targets. Identification and location of a jammer are implemented by maintaining a history of the ambient noise level. When that level increases significantly at a given bearing, it may be assumed that a jammer exists at that bearing. Thresholding and integration length for this technique are dependent upon antenna pattern characteristics and antenna scan rate. However, if the jammer level is sufficient to cause degradation, it will always be detectable by this technique.

In the simplest scenario, the enemy is ignorant of the instantaneous frequency used by the victim radar. However, from intelligence data, the basic band of operation is known almost always. In this case, the jammer has little choice but to spread its energy over this entire band. This frequency dilution requires fairly high power levels. In advanced scenarios, the enemy must be given credit for the ability to measure the instantaneous frequency radiated by the victim. Then, jamming energy may be concentrated at that frequency with a consequent reduction in required power level. This is referred to as *spot jamming*.

Suppose that the victim radar operates somewhere within an allocated band of 500 MHz but that the instantaneous radiated and received bandwidth is only 5 MHz. The barrage jammer would have to radiate noise over the entire 500 MHz but the spot jammer bandwidth would need be only 5 MHz. The advantage would be a factor of 100 or 20 dB.

Spot jamming may be countered by frequency agility within the victim radar. Because there is a fairly large range separation between radar and ECM system, there will be a finite time delay between radiation initiation from the victim and sensing of that radiation at the ECM system. An additional delay results from the finite tuning time required for

the spot ECM system to change frequency. During the sum of these delays, the victim radar enjoys a noise-free target dwell. If the victim changes frequency after a given delay, the ECM system cannot keep up, and the victim is free to detect targets.

A final ECM technique is termed *deception*. Here, the ECM system receives the victim-radiated pulse and reradiates that pulse with a time delay or Doppler shift. The victim radar thus receives two signals. One is the true target reflection and one is a false target return. Through clever manipulation of the time delay or Doppler shift, the ECM may be successful in decoying the radar to assign a weapon to the false target and, thus, to waste ammunition. However, because this technique does not hide the true target return, its benefit is highly questionable. This rather complex ECM method is not in common practice against search radars due to its lack of real cost-effectiveness. It is much more useful against dedicated tracking radars where it may effect stealing of range and velocity tracking loops.

Radar Frequency Interference

There are a large number of radars in operation worldwide. It is likely that several of these systems may be located in close proximity. Because the one-way propagation loss between two systems falls off at only R^2, one radar may detect the direct radiation from another. The result is termed *radar frequency interference* (RFI).

Radar frequency interference may be categorized into two classes. The first class involves two or more radars of the same type. These are designed for the same function, by the same design team, and produced by the same manufacturer. An example is a fleet of ships where each ship carries its own search radar. The second class involves radars of dissimilar type. These have different functions and, probably, have been produced by different companies. An example might be an airport installation using one high-power general surveillance radar and one or more lower power radars to monitor take-offs and landings.

To minimize RFI, the federal government issues licenses, establishes regulations, and allocates frequency bands to every radio, television, and radar system deployed within the United States. Other nations have similar functions. Control is extended to all radiating systems including experimental and developmental models.

When two radars in close proximity are of the same type, the designer has some control over RFI. The first defense is channelization. The radar system may be allocated, for example, a total band of 1000 MHz but its instantaneous radiated bandwidth might be only 10 MHz. Assignment of separate channels spaced by 10 MHz to each particular radar would allow 100 systems to operate simultaneously without any two being in the same channel. Unfortunately, channelization does not completely solve the RFI problem. The radiated spectrum of a rectangular pulse has very significant energy many bandwidths removed from the carrier frequency. This energy can enter the victim receiver and cause interference.

A second defense is PRF diversity. When two radars operate at the same PRF, the received pulses from the interferer integrate normally and, probably, create a detection. When two different PRFs are used, the integration is negated and the RFI effect is reduced by a factor equal to the integration length. This is not a total panacea. Selection of PRF is a delicate process involving questions of blind ranges, blind velocities, and range ambiguity resolution. In a given application, there may not be a sufficient band of usable PRFs to serve multiple radars. Moreover, diversity may even compound the problem. If an interference pulse is sufficiently strong, it may be detectable without integration. This pulse will migrate over many range cells and produce multiple detections. This could result in a swarm of false targets that might overcome the correlation capability of the system computer.

Neither of the techniques discussed above is applicable to the class involving radars of different types. In this case, the only viable defense appears to be asynchronous pulse detection (APD). In the APD technique, successive pulses in a given range cell are compared. If the later pulse is much larger than the earlier pulse, it is edited from the data stream and replaced by either the earlier sample or a random number. Of course, this approach works only when two different PRFs are involved. Asynchronous pulse detection can be very effective in minimizing RFI. However, depending upon the thresholding scheme employed, it can cause degradation in the detectability of real targets.

ADVANCED DESIGN

In this section, topics are discussed that represent potential performance improvements to future designs. However, none of these are new innovations. The concepts have been known and understood for many years. As technology evolves, though, these techniques become more and more cost effective and attractive to the designer of advanced systems.

Phased Array Antennas

Phased array antennas are planar arrays of waveguide slots. Variable phase shifters are used to drive a group of slots and, thus, to effect electronic steering of the antenna beam. This technique can eliminate the necessity for bulky mechanical devices such as motors and gimbaled platforms.

The basic theory of phased arrays is described best by considering the simplest case, which is a two-element array. The radiated fields from two adjacent sources combine in space to form a radiation pattern. When a phase shift is applied to one element, the directivity of that pattern may be altered. In this simple case, it may be shown that the relative gain of the array is

$$G = \frac{2 + 2\cos(\pi \sin\alpha - \phi)}{4}$$

where α is the space angle relative to perpendicular and ϕ is the introduced phase shift. Maximum gain occurs when

$$\alpha = \sin^{-1}(\phi/\pi)$$

Thus, for small angles, the ratio of phase shift to steered angle is approximately a factor of three. In no way does this example present the design equations for a complex array. It simply shows the effect of phase shift on boresight shift.

The concept is extended easily to linear arrays of any length, N, and to two-dimensional arrays having $N \times M$ elements (9). In practice, the pattern produced by an array will

be the product of the pattern from each element and the array factor, which is determined by the element spacing. The optimum spacing is one-half wavelength. At wider spacing, the pattern begins to develop unwanted sidelobes called grating lobes. These can be as large as the main lobe and may cause confusion or interference. In addition, coupling between elements can alter the actual antenna pattern. Phased array design is a complex process.

When the array beam is steered off-axis, the beam will broaden and the gain will decrease. In general, this effect is in proportion to the cosine of the steered angle. For example, a steering angle of 45° may result in a loss of 1.5 dB relative to on-axis gain.

When the element spacing is one-half wavelength, the number of elements and required phase shifters can become quite large. For example, consider a design at *X* band where one wavelength is 0.03 m. An antenna 1 m on a side would require 4356 phase shifters to enable steering in both planes. The sheer cost and weight of this system might be prohibitive.

A good compromise design is one in which the antenna array is rotated mechanically in azimuth while being steered electronically in elevation. The example given previously would then require only approximately 66 phase shifters to provide elevation-only steering. This approach also allows for raster scanning. Rather than holding the elevation position constant over a full 360° rotation, the beam could be directed to visit several elevation positions during one scan. This not only reduces the time required to illuminate a given volume but, since the beam traverses the target in both dimensions, beam splitting in elevation and azimuth could be implemented.

An ultimate phased array design is the conformal array. Here, the array is designed as an integral part of an existing geometry. That geometry might be the fuselage or wing of an aircraft or the hull of a ship. The ideal conformal array would be a sphere or hemisphere. This design could eliminate off-axis steering loss, because the beam would always be perpendicular to the array surface.

Another advantage of phased arrays is their capability for instant target verification. An initial detection could be followed by freezing the beam in the direction of the target detection. Then, a longer dwell could be chosen to both reduce measurement error and increase confidence level. The time savings relative to scan-to-scan verification could be significant.

A final application of phased arrays is in platform motion compensation. When the radar is carried by an aircraft or ship, it is desirable that the beam position be maintained relative to earth coordinates independent of platform motion. This is implemented easily using beam steering and its use eliminates the necessity for complex motor-gimbal apparatus.

Active Arrays

The next generation of search radar may well use the concept of the active array. This is a natural extension of the phased array. In that design, each array element is provided with its own transmitter and receiver module. This solid-state module contains a low-power transmission amplifier, receiver protection, a low-noise RF preamplifier, filtering, and frequency conversion. It also contains a digitally controlled phase shifter for beam control. On transmission, all modules are driven by the same coherent signal from a frequency synthesizer. That element also provides one or more local oscillator signals for frequency conversion to IF. The IF signals are combined to form one channel for signal processing.

A chief advantage of the modular array is the elimination of a large, expensive, hard-tube transmitter. Its disadvantage is in the huge number of modules required. If 4356 elements are required, then that number of modules is also required. If the cost of each module were only $100, then the total array cost would approach $500,000. For this reason, the modular array has not found a large application. However, as technology improves and costs decrease, this approach may become very popular in future designs.

Discrete Fourier Transform

The discrete Fourier transform (DFT) is a digital signal processing technique that provides perfect, coherent integration of incoming pulse trains and filter discrimination among target and clutter Doppler shifts. Usually, it is implemented as a bank of equally spaced digital filters that spans a frequency band equal to the PRF. The response of a given filter repeats at integral multiples of the PRF.

These filters are generated by summing the product of the incoming samples with a time-varying sequence of coefficients. The latter is designed to produce a narrowband filter at some prescribed frequency. The output of a given filter is

$$F = \sum_{n=0}^{N-1} A[\cos 2\pi fnT_r + j \sin 2\pi fnT_r] \times [\cos 2\pi f_c nT_r - j \sin 2\pi f_c nT_r]$$

where A is the peak amplitude of the input signal, f is the frequency of the input signal, f_c is the center frequency of the filter and T_r is the pulse repetition interval. N is the number of pulses integrated. Note that the input and coefficient sequences are expressed as complex quantities. The real part of the input is taken from the in-phase video channel, whereas the imaginary part is taken from the quadrature. The output is also complex valued.

The real, or in-phase, output may be shown to be

$$F_i = \sum_{n=0}^{N-1} A \cos 2\pi(f - f_c)nT_r$$

and the imaginary, or quadrature, output is

$$F_q = \sum_{n=0}^{N-1} A \sin 2\pi(f - f_c)nT_r$$

When the input signal frequency coincides with the filter center frequency, the outputs are

$$F_i = NA$$

and

$$F_q = 0$$

The square of the output magnitude, which is output power, is, then,

$$M^2 = F_i^2 + F_q^2 = N^2A^2$$

The filter response to noise is given by

$$F = \sum_{n=0}^{N-1} [x_n + jy_n][\cos 2\pi f_c n T_r - j \sin 2\pi f_c n T_r]$$

where x_n and y_n are noise samples taken from the in-phase and quadrature channels, respectively. These samples are assumed to be independent from channel to channel and sample to sample. They have a Gaussian probability distribution with zero mean and variance σ^2. The in-phase output is

$$F_i = \sum_{n=0}^{N-1} x_n \cos 2\pi f_c n T_r + y_n \sin 2\pi f_c n T_r$$

The variance of that output is

$$\begin{aligned} V(F_i) &= \sum_{n=0}^{N-1} V(x_n)\cos^2 2\pi f_c n T_r + V(y_n)\sin^2 2\pi f_c n T_r \\ &= \sum_{n=0}^{N-1} \sigma^2[\cos^2 2\pi f_c n T_r + \sin^2 2\pi f_c n T_r] = N\sigma^2 \end{aligned}$$

It may be shown also that

$$V(F_q) = N\sigma^2$$

Then, the output SNR is

$$\mathrm{SNR}_0 = \frac{N^2 A^2}{2N\sigma^2} = N\frac{A^2}{2\sigma^2} = N \cdot \mathrm{SNR}_i$$

where SNR_i is the input, per-pulse SNR. Thus, the DFT provides an SNR gain equal to the length of integration. For example, if that length was 100, the gain would be a very impressive 20 dB. No other known technique yields a higher SNR gain than the DFT.

The normalized frequency response of the DFT filter may be shown to be

$$G_{\mathrm{norm}} = \left[\frac{\sin N\phi}{N \sin \phi}\right]^2$$

where

$$\phi = \pi f / f_r$$

f is frequency relative to filter center frequency and f_r is the PRF. This response is plotted in Fig. 8 for the case $N = 10$. In this plot, a frequency normalization factor, k, is used. When $k = 0, f = 0$ and when $k = 1, f = f_r$.

It will be noted that the response exhibits sidelobes. The first sidelobe is 13 dB below the main lobe response. Also, note that the response repeats at integral multiples of the PRF.

If the relatively high sidelobes are not sufficient to provide desired clutter attenuation, then window functions may be applied to suppress these sidelobes. A window function is a real-valued, time-varying sequence applied to the input data for all filters. With a window, the DFT response is given by

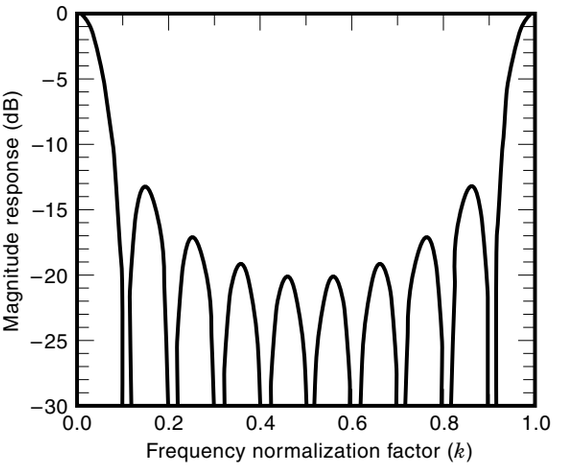

Figure 8. Frequency response of a discrete Fourier transform filter with uniform window. The DFT response is relatively narrow but exhibits sidelobes, which may cause extraneous detections.

$$F = \sum_{n=0}^{N-1} AW(n)[\cos 2\pi f n T_r + j \sin 2\pi f n T_r] \\ [\cos 2\pi f_c n T_r - j \sin 2\pi f_c n T_r]$$

where $W(\ )$ is the window function. A typical function is

$$W(n) = \sin^2\left(\frac{\pi n}{N}\right)$$

which reduces the first sidelobe to a level approximately 32 dB below the main lobe response. There is almost an infinite number of windows that might be applied in a given application. Harris (10) presents an entire catalog of windows and lists advantages and disadvantages.

The use of windows is not without penalty. Invariably, the main lobe gain will be reduced and the bandwidth will be increased. Thus, a trade-off exists between sidelobe response and main lobe performance.

The DFT dwell length is

$$T_d = NT_r$$

and the filter bandwidth is, roughly,

$$B = \frac{f_r}{N} = \frac{1}{T_d}$$

Normally, the nominal number of filters implemented is equal to the integration length, N. Then, the filter spacing is almost equal to the bandwidth. This is not an inviolable rule. When the number of filters exceeds N, the loss to frequencies between filter centers is reduced but the filter outputs are correlated somewhat. Fewer filters result in more loss.

A very interesting signal processing scheme is the one in which a nonrecursive MTD is used preceding the DFT. This type of MTD, which does not employ feedback, has the very attractive feature that no transients are produced when radar frequency is changed, beams are transitioned, or PRF is changed. Thus, wasteful receiver blanking is avoided. This feature is achieved because the combined MTD–DFT re-

sponse is constant over most of the PRF bandwidth. Although the MTD attenuates low-frequency signals, it also attenuates noise in their vicinity within the narrow DFT bandwidth. The result is an almost constant SNR over most of the band covered. Thus, the combined response can be made to approximate that of a well-designed MTD with feedback, but transients will be absent. Wilson (11) presents a derivation of SNR loss using this combination.

Clutter Tracking

In many applications, shipboard and airborne, the radar platform is in motion. In these cases, the received clutter Doppler may be nonzero and its spectrum may not be canceled sufficiently in the relatively narrow null of the MTD response. Improved clutter rejection may be obtained by incorporating a clutter tracker. This subsystem measures the clutter Doppler and, through various tuning schemes, positions the clutter spectrum exactly at the MTD null for maximum suppression. The clutter tracker is a special purpose, automatic frequency control (AFC) loop.

Archaic designs might use analog frequency discriminators for clutter frequency sensing. However, a preferred approach is to use a pair of DFT filters. One filter is centered at some frequency below clutter and the other is centered above. An almost linear error function is obtained by forming the following ratio:

$$\epsilon = \frac{F_{\mathrm{l}}(f) - F_{\mathrm{h}}(f)}{F_{\mathrm{l}}(f) + F_{\mathrm{h}}(f)}$$

where F_{l} and F_{h} are the frequency responses of the lower and higher filters, respectively. The spacing of the filters and the required integration length are dictated by the clutter scenario and geometry. The AFC loop is used to drive this error to 0 where maximum cancellation is achieved.

Tuning of the clutter spectrum may be achieved using a variable frequency oscillator as the final local oscillator. That approach is discouraged, because free-running oscillators tend to be noisy and, invariably, produce unwanted intermodulation products within the video bandwidth. A more attractive option is to tune the MTD itself using digital control. As an example, consider the first-order canceler. Without tuning, its output is given by

$$F_0 = g(n) - g(n-1)$$

where $g(n) = \cos(2\pi f T_{\mathrm{r}}) + j \sin(2\pi f T_{\mathrm{r}})$, f is the Doppler frequency, and T_{r} is the repetition interval. This function may be shown to have a null at zero frequency. Tuning is accomplished by multiplying the delayed pulse by a complex constant. Thus,

$$F_0 = g(n) - [\cos\phi_1 + j \sin\phi_1]\, g(n-1)$$

where $\phi_1 = 2\pi f_1 T_{\mathrm{r}}$. It may be shown that the null of this function has been shifted to f_1.

When using cancelers having multiple delays, two or more separate nulls may be obtained. This would be useful, for example, in placing sea clutter and rain clutter, which are separated in Doppler, into their own nulls. Of course, the design of a dual-frequency AFC loop does present a challenge. Because the clutter Doppler oscillates as the antenna bearing angle rotates relative to the platform velocity vector, tracking may be aided by introducing antenna angle into the AFC loop. With this aid, the tracking loop can be a simple, first-order implementation which is not required to compensate for Doppler accelerations introduced by rotation. Wilson (12) suggests an adaptive clutter tracking algorithm.

Post Discrete Fourier Transform Integration

In the usual implementation of the DFT, one electronic module is assigned to each center frequency, and that module processes all range cells within the repetition interval. Current technology allows these modules to be designed as integrated circuits using VLSI. Although each module is very small, the sheer number required can place a severe strain on available signal processor real estate. Also, there is, a cost impact. Thus, there will be a limitation on the number of filters available.

Given that the number of filters is limited to N_{f}, then the spacing between filters is PRF/N_{f}. However, a particular target Doppler may fall midway between centers. As the integration length increases, the bandwidth of each filter decreases and a loss is imparted to the midway signal. Thus, there is an optimum integration length that maximizes the SNR gain for that signal. It may be shown that the optimum length is 0.74 N_{f} for an unweighted DFT.

In many applications, the available pulses during a beam dwell will far exceed the optimum integration length. For example, with a beamwidth of 5°, a scan rate of 60 RPM and a PRI of 30 μs, the number of pulses over the beam is approximately 463. If only 50 filters were implemented, the optimum DFT length would be 37. Thus, there would be 12 or 13 DFT outputs per beam position. The careful designer should try to combine these outputs into a single decision. This combining requires post-DFT integration.

The post-DFT integrator might be a Markov chain, which is a simple and effective approach. However, the magnitude integrator has superior performance. In that approach, individual DFT output magnitudes are summed and the result applied to a threshold test. The only disadvantage to this technique is that probability of false alarm is difficult to predict. Apparently, the only viable means for predicting false alarm characteristics is by Monte Carlo simulation.

Another aspect of magnitude integration is block versus sliding integration. In the block integrator, several DFT outputs are allowed to accumulate before thresholding. Then, another block is collected. In this approach, it may turn out that both blocks lie on the beam skirts and full benefit of main bean gain is not achieved. A preferred approach is to allow the DFT summation to slide across the beam where a new sum is produced after each DFT on a first-in, first-out basis. This requires more computer memory but ensures that at least one block will encompass the maximum antenna gain.

BIBLIOGRAPHY

1. M. I. Skolnik, *Introduction to Radar Systems,* New York: McGraw-Hill, 1962, pp. 3–5.
2. M. I. Skolnik (ed.), *Radar Handbook,* New York: McGraw-Hill, 1970, pp. 9-1, 9-40.
3. M. Schwartz, *Information Transmission, Modulation, and Noise,* New York: McGraw-Hill, 1959, pp. 282–291.

4. M. Schwartz, *Information Transmission, Modulation, and Noise,* New York: McGraw-Hill, 1959, pp. 392–413.
5. D. D. Monahan, Average Time Between False Alarms for Phalanx Block I in Low PRF, TM#6-257-851, Pomona, CA: General Dynamics Corporation, 1985.
6. M. I. Skolnik, *Introduction to Radar Systems,* New York: McGraw-Hill, 1962, pp. 462–482.
7. F. E. Nathanson, *Radar Design Principles,* New York: McGraw-Hill, 1969, pp. 228–275.
8. M. I. Skolnik (ed.), *Radar Handbook,* New York: McGraw-Hill, 1970, pp. 17-1, 17-60.
9. M. I. Skolnik, *Introduction to Radar Systems,* New York: McGraw-Hill, 1962, pp. 294–320.
10. F. J. Harris, On the use of windows for harmonic analysis with the discrete Fourier transform, *Proc. IEEE,* **66**: 51–83, 1978.
11. D. J. Wilson, Signal-to-Noise Ratio Loss in a Combined Clutter Canceler-DFT Signal Processor, IC#5G41.10/003/DJW, Tucson, AZ: Hughes Missile Systems Company, 1994.
12. D. J. Wilson, A Clutter Adaptive Algorithm for the Phalanx Upgrade Search Radar, IC#5G41.10/010/DW, Tucson, AZ: Hughes Missile Systems Company, 1995.

DUSTIN J. WILSON
Hughes Missile Systems Company
(retired)

SECOND-ORDER CIRCUITS. See TRANSIENT ANALYSIS.
SEEBECK EFFECT. See PELTIER EFFECT.
SEEBECK EMF. See THERMOCOUPLES.
SEGMENTATION, IMAGE. See IMAGE SEGMENTATION.
SEISMIC DATA PROCESSING. See GEOPHYSICAL SIGNAL PROCESSING.